



Measurement report: Long-term measurements of ozone concentrations in semi-natural African ecosystems

Hagninou Elagnon Venance Donnou¹, Aristide Barthélémy Akpo¹, Money Ossohou^{2,3}, Claire Delon⁴,
5 Véronique Yoboué³, Dungall Laouali⁵, Marie Ouafou-Leumbe⁶, Pieter Gideon Van Zyl⁷, Ousmane
Ndiaye⁸, Eric Gardrat⁴, Maria Dias-Alves⁴, and Corinne Galy-Lacaux⁴

¹Laboratoire de Physique du Rayonnement, Faculté des Sciences et Techniques,
Université d'Abomey-Calavi, Cotonou, 01 B.P. 526, Benin

10 ²Department of Physics, University of Man, Man, Côte d'Ivoire

³Laboratoire des Sciences de la Matière, de l'Environnement et de l'Energie Solaire,
Université Félix Houphouët-Boigny, Abidjan, Côte d'Ivoire

⁴Laboratoire d'Aérodynamique, Université Toulouse III Paul Sabatier, CNRS, Toulouse, 31400, France

15 ⁵Laboratoire de Climat-Environnement et Matériaux-Rayonnement, Université Abdou Moumouni,
Faculté des Sciences et Techniques, Niamey, BP 10662, Niger.

⁶Department of Earth Sciences, Faculty of Sciences, University of Douala, Douala, P.O. Box 2701, Cameroun

⁷Atmospheric Chemistry Research Group, Chemical Resource Beneficiation, North-West University,
Potchefstroom, 2520, South Africa

⁸Centre de Recherches Zootechniques de Dahra, Institut Sénégalais de Recherches Agricoles, Dahra, Senegal

20

Correspondence to: H. E. Venance Donnou (donhelv@yahoo.fr) and Corinne Galy-Lacaux (corinne.galy-lacaux@aero.obs-
mip.fr)

Abstract. In the framework of the International Network to study Deposition and Atmospheric chemistry in Africa (INDAAF)
25 program, we present the seasonal variability of atmospheric ozone concentrations at the regional scale. The contributions of
local atmospheric chemistry and meteorological parameters to ozone photochemistry are investigated, as are long-term trends
in ozone concentrations. Fourteen measurement sites were identified for this study, representative of the main African
ecosystems: dry savannas (Banizoumbou, Niger, Katibougou and Agoufou, Mali, Bambey and Dahra, Senegal), wet savannas
(Lamto, Côte d'Ivoire, Djougou, Benin), forests (Zoétélé, Cameroon, Bomassa, Republic of Congo) and semi-agricultural/arid
30 savanna (Mbita, Kenya, Louis Trichardt, Amersfoort, Skukuza and Cape Point, South Africa). Over the period 1995-2020,
monthly ozone concentrations were measured at these sites using passive samplers. Monthly averages of surface ozone range
from 4.7 ± 1.4 ppb (Bomassa) to 31.0 ± 10.5 ppb (Louis Trichardt). Ozone levels in the wet season (in dry savanna) are higher
and comparable to concentrations in the dry season (in wet savanna and forest). In East Africa, ozone levels show no marked
seasonality, with higher levels in Southern Africa. In the Sahel, under the influence of temperature, ozone formation is closely
35 linked to biogenic Volatile Organic Carbon (VOC) emissions. It is also sensitive to nitrogen monoxide (NO) emissions in the
presence of high precipitation and humidity. Biogenic VOC (BVOC) emissions, anthropogenic NO_x, temperature and radiation
are the dominant contributors to O₃ formation in wet savannas and forests. At the southern African sites, the most important
parameters influencing surface ozone concentrations are humidity, temperature, VOC emissions (anthropogenic and biogenic)
and NO_x. At the annual scale, Katibougou and Banizoumbou sites (dry savanna) experienced a significant decrease in ozone
40 concentrations respectively around -0.24 ppb yr⁻¹ (-2.3 % yr⁻¹) and -0.15 ppb yr⁻¹ (-1.9 % yr⁻¹). Seasonal Kendall statistical
tests revealed decreasing trends of -0.07 ppb yr⁻¹ in Banizoumbou and -0.24 ppb yr⁻¹ in Katibougou. These decreasing trends
are consistent with those observed for nitrogen dioxide (NO₂) and biogenic VOCs. A significant increasing trend is observed



45 in Zoétélé, with the Sen slope estimated at 0.1 ppb yr^{-1} and at Skukuza (Sen slope = 0.3 ppb yr^{-1}). The increasing trends are consistent with the increase in biogenic emissions at Zoétélé and NO_2 levels at Skukuza. Very few surface O_3 measurements exist in Africa, and long-term results presented in this study are the most extensive for the studied ecosystems.

1 Introduction

Ozone (O_3) is a greenhouse gas, difficult to observe and quantify on a global scale due to its acute spatial variability resulting from its variable photochemical lifetime (between 20 and 25 days) (Cooper et al., 2020; Young et al., 2013). It has phytotoxic effects altering key plant physiological processes that can significantly reduce the productivity of agricultural crops and ecosystems (Dufour et al., 2021; Lelieveld et al., 2015; Mills et al., 2018; Monks et al., 2015). At the local scale, its presence in high concentrations in the lower troposphere is harmful to human health, notably through irritation of the upper airways (Camredon and Aumont, 2007; Schultz et al., 2017). O_3 is a secondary air pollutant, meaning that it is not emitted directly but formed in the troposphere as a result of oxidative chemical reactions of precursor gases such as nitrogen oxides (NO_x), carbon monoxide (CO) and volatile organic compounds (VOCs) (Lu et al., 2019; Schultz et al., 2017). It is chemically lost by photodissociation or by surface deposition and uptake by plant stomata (Silva and Heald, 2018), or by heterogeneous reactions involving aerosols. Stomatal uptake of O_3 and subsequent damage to plants can lead to changes in biosphere-climate interactions (Sadiq et al., 2017). Mitigating its negative impacts on health requires reducing both pollutant concentrations and population exposure (Petetin et al., 2022). These changes are compounded by the variation of O_3 precursors, which in recent decades have shifted from high and mid-latitudes to low latitudes, where O_3 production efficiency is greater (Zhang et al., 2016). These variations are particularly significant in tropical regions, where seasonal cycles linked to natural and anthropogenic sources of gas and particle emissions are well marked (Adon et al., 2010). Air quality forecasts could therefore be used to warn the population of the potential occurrence of a pollution episode (Petetin et al., 2022). Its long-term importance for atmospheric chemistry has been investigated by several studies on air quality (Monks and Leigh 2009) and atmosphere-biosphere interactions (Fowler et al., 2009; Laban et al., 2018).

International Global Atmospheric Chemistry Project (IGAC) has produced the Tropospheric Ozone Assessment Report (TOAR) on the global Measures for Climate Change, Human Health and Crop/Ecosystem Research (www.igacproject.org/TOAR). This report stated that free tropospheric O_3 has increased during the industrial era and in recent decades (Gaudel et al., 2018; Tarasick et al., 2019). Despite these years of regional and global surface O_3 research and monitoring, many regions of the world such as Africa, South America, the Middle East and India, remain under sampled, leading to incomplete knowledge of the horizontal, vertical and temporal distribution of O_3 (Cooper et al., 2014; Lin et al., 2015; Mills et al., 2018; Oltmans et al., 2013; Sofen et al., 2016). Although Africa is considered as one of the most sensitive continents to air pollution and climate change, it is the least studied (Laakso et al., 2012; Swartz et al., 2020a). Indeed, very little work has been done on regional atmospheric chemistry and the dominant atmospheric processes related to surface O_3 formation in Africa. With the exception of a few sites, O_3 variability is not yet sufficiently documented on this continent (Gaudel et al., 2018; Fleming et al., 2018; Mills et al., 2018).

From this perspective, long term measurement programs play a vital role in studies of air pollution and the various changes in the chemical composition of the atmosphere. These long-term assessments are crucial for posing the most topical research questions on atmospheric chemistry (Vet et al., 2014), in order to provide the right answers for relevant decision-making at local and global scale. In situ, satellite, O_3 -sonde and aircraft observations provide a substantial amount of information on the current distribution of tropospheric O_3 , its variability and trends (Gaudel et al., 2018; Tarasick et al., 2019). They are well suited to improve our understanding of emissions, transport, chemical reactions, deposition processes and the impacts of atmospheric species on human health, vegetation and climate change (Lefohn et al., 2018). Numerous projects and programs have therefore sprung up in several places around the world, for decades.

85 In Africa, the International Network to Study Deposition and Atmospheric Composition in Africa (INDAAF; <https://indaaf.obs-mip.fr>), operational since 1995, is dedicated to study the evolution of the chemical composition of the



90 atmosphere and deposition fluxes. INDAAF is a national observatory (Service National d'Observation, SNO) of the Institut National des Sciences de l'Univers (INSU) of the Centre National de Recherche Scientifique (CNRS) and of the Institut de Recherche pour le Développement (IRD), and a labelled component of the European research infrastructure Aerosols, Clouds and Trace gases Research Infrastructure (ACTRIS). The INDAAF long term monitoring network is also labelled by Global Atmosphere Watch (GAW) program of the World Meteorological Organization (WMO) as a contributing network and is a component of the DEBITS (Deposition of Biogeochemically Important Trace Species) activity of IGAC (International Global Atmospheric Chemistry).

95 Previous existing studies have considered surface ozone levels in Africa. Adon et al. (2010) characterized the ozone concentration levels (together with several atmospheric pollutants), from 2002 to 2007, at seven remote sites in West and Central Africa, while Martins et al. (2007) investigated O₃ concentrations in Southern Africa over a period of 9 to 11 years (1995-2005). In South Africa, Swartz et al. (2020a) assessed long-term seasonal and interannual trends of O₃ based on a 21-years (1995-2015) dataset at the Cape Point station. This work was continued at 3 historic IDAF-DEBITS sites (Amersfoort, Louis Trichardt, Skukuza, Swartz et al., 2020b). Laban et al. (2018) reported O₃ levels in northeastern South Africa, and 100 characterized the links between observed NO_x and O₃ concentrations. Other works were carried out by Bencherif et al. (2020), Gaudel et al. (2020), Hamdun and Arakaki (2015), Ihedike et al. (2023), Josipovic et al. (2010), Khoder (2009), Lee et al. (2021), Ngoasheng et al. (2021), Zunckel et al. (2004) in different locations in Africa to characterize O₃ pollution levels. Other projects such as POLCA (POLlution des Capitales Africaines) and DACCIWA (Interactions Dynamique-Aérosols-Chimie-Nuages en Afrique de l'Ouest), have also been implemented in African capitals such as Bamako, Dakar and Yaoundé (Adon 105 et al., 2016), Abidjan, Cotonou (Bahino et al., 2018) and have provided O₃ concentration surface measurements.

However, very little information is available on the long-term evolution of O₃ chemistry in Africa. The impact of meteorological parameters (temperature, humidity, rainfall, radiation) and atmospheric chemistry (NO_x and VOCs concentrations) on the seasonality of O₃ concentrations, and the analysis of long-term O₃ trends remain unexplored. Further work is therefore needed to fill the data gaps in Africa, and better understand the mechanisms of O₃ formation as a function of 110 ecosystems and their long-term evolution.

As part of the INDAAF program, this study aims to improve the long-term assessment of surface O₃ in the western, central, eastern and southern African regions. In the first objective, we first document the long-term (1995-2020 depending on the site) monthly, seasonal and interannual variability of O₃ concentrations on a regional scale at fourteen sites grouped by ecosystem (dry savannas, humid savannas, forests and agricultural/semi-arid savannas), followed by a comparative study with existing 115 references. The study goes further by discussing the seasonal architecture of anthropogenic and biogenic O₃ precursors based on meteorological parameters and emission inventories. In the second objective, we study the impact of meteorological parameters (temperature, humidity, precipitation, radiation) and atmospheric chemistry precursors (NO_x and VOC) on photochemical O₃ production, using principal component analysis. In this section, we establish the correlation matrix between O₃, its gaseous precursors and meteorological parameters. An attempt is made to assess their different contributions to 120 photochemical O₃ production in each ecosystem. In the third objective, we use non-parametric statistical tests to assess long-term seasonal and annual trends in O₃, and discuss the results according to trends in anthropogenic and biogenic emissions of precursors. For the first time, the chemical evolution of tropospheric O₃ is examined over the long term at all INDAAF and companion sites. This study provides a robust regional mapping of the long-term seasonal cycle O₃ formation at the continental scale.

125 2. Materials and methods

2.1 Sampling sites

Fourteen O₃ measurement sites located in different African ecosystems have been selected for this long-term study of tropospheric O₃ chemistry (Fig. 1), among which 8 stations of the INDAAF long-term monitoring network located in 7 West 130 and Central Africa countries (Mali, Niger, Ivory Coast, Senegal, Benin, Congo and Cameroon). These sites are characteristic



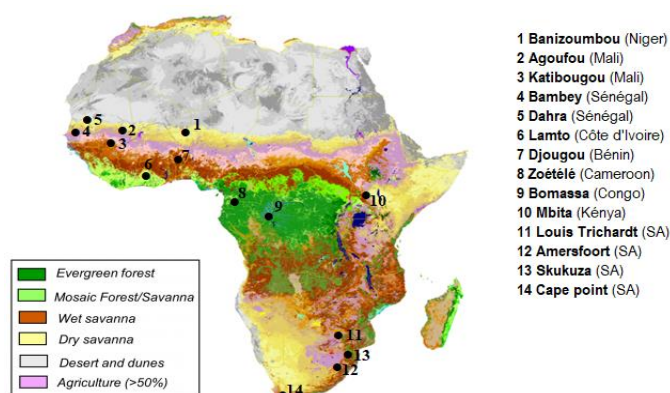
of dry savanna, humid savanna and forest ecosystems (Table 1). A detailed description of INDAAF monitoring stations and land use classes is available in Adon et al. (2010, 2013). Other sites implemented through INDAAF’s companion projects and using the same O₃ measurements protocols were also selected for this study. The site of Dahra in Senegal, part of the ‘Cycle de l’Azote entre la Surface et l’Atmosphère en afriQUE’ (CASAQUE) project is located in dry savanna and used for grazing (Bigaignon et al., 2020). The site of Mbita, part of the Integrated Nitrogen Management system (INMS) is located in East Africa. In South Africa, four long-term DEBITS sites (Louis Trichardt, Skukuza, Cape Point and Amersfoort) are considered. They are regionally representative of the specific ecosystems of southern Africa. Full descriptions of these South African sites can be found in the works of Conradie et al. (2016), Laakso et al. (2012) and Swartz et al. (2020a,b). All study sites are representative of semi natural rural sites in remote regions. Table 1 presents geographical coordinates and some ecological and climatological characteristics of the sites. In the remainder of the text, the measuring stations will be referred to using the following abbreviations: Banizoumbou (Ba), Katibougou (Ka), Agoufou (Ag), Bambey (Bb), Dahra (Da), Lamto (La), Djougou (Dj), Zoetele (Zo), Bomassa (Bo), Mbita (Mb), Louis Trichardt (LT), Skukuza (Sk), Cape Point (CP) and Amersfoort (Af).

Table 1. Geographical, ecological and climatic characteristics of the study sites

Ecosystem	Station	Latitude, Longitude	Country	Land cover classes	Climate
Dry savanna	Banizoumbou (Ba)	13°18' N, 02°22' E	Niger	Open grassland with sparse shrub and culture	Sahelian
	Katibougou (Ka)	12°56' N, 07°32' W	Mali	Deciduous shrubland with sparse trees	Sudano-Sahelian
	Agoufou (Ag)	15°20' N, 01°29' W	Mali	Open grassland with sparse shrub and trees	Sahelian
	Bambey (Bb)	14°42' N, 16°28' W	Senegal	Cultivated grass land with sparse trees	Sahelian
	Dahra (Da)	15°24' N, 15°26' W	Senegal	Open grassland with sparse shrub and trees, sylvopastoral area	Sahelian
Wet savanna	Lamto (La)	06°13' N, 05°02' W	Cote d'Ivoire	Mosaic forest/savanna	Guinean
	Djougou (Dj)	09°39' N, 01°44' E	Benin	Deciduous open woodland	Sudano-Guinean
Forest	Zoetele (Zo)	03°10' N, 11°49' E	Cameroun	Dense evergreen	Guinean
	Bomassa (Bo)	02°12' N, 16°20' E	Congo	lowland forest	Guinean
Agricultural field	Mbita (Mb)	0°25' S, 34°12' E	Kenya	Tropical agricultural area	Subtropical
	Louis Trichardt (LT)	22°59' S, 30°01' E		Cultivated/Semi-arid regional savanna	Subtropical
	Skukuza (Sk)	24°59' S, 31°35' E		Semi-arid regional background site surrounded by natural bushveld in a protected area Southern	Subtropical



Regional savanna/ Semi-arid	Cape Point (CP)	34°21' S, 18°29' E	South Africa	Hemispherical marine background site, rocky and sparsely vegetated, Fynbos biome Semi-arid regional savanna, impacted by anthropogenic activities	Mediterranean Warmtemperate
	Amersfoort (Af)	27°04' S, 29°52' E			



150 **Figure 1.** Location of the 14 measurement studied sites in Africa on a vegetation map (adapted from Mayaux et al., 2004)

2.2 Passive sampling and chemical analysis

O₃ concentrations were measured using passive samplers developed at the Laboratoire d'Aérodologie (LAERO) in Toulouse in the framework of the INDAAF program, and at the North West University in Potchefstroom in South Africa. They are based on the passive sampling technique, which relies on laminar diffusion and the chemical reaction of the atmospheric pollutant under consideration (Adon et al., 2010; Ferm, 1991 and Martins et al., 2007). These sensors have been tested and validated in different tropical and subtropical regions (Carmichael et al., 2003; Martins et al., 2007). The measurement protocols including passive samplers deployment, analysis by Ionic chromatography and the calculation method of concentrations have been widely described in previous studies (Adon et al., 2010; Bahino et al., 2018; Carmichael et al., 2003; Ferm and Rodhe, 1997; Galy-Lacaux et al., 2009; Galy-Lacaux and Modi, 1998; Ossouhou et al., 2019; Swartz et al., 2020b). In this paper, we use monthly database of O₃ concentrations. The concentration measurement period runs from the start date of measurements at each site to 2015-2020 (Table 2). O₃ concentration collection efficiency on the sampling period (ratio of the number of valid concentrations to the number of filters analysed) was assessed at each of the 14 sites (Table 2). All wet and dry seasons duration are indicated in Table 2. These proportions are fairly representative of high quality measurements as indicated in the work of Laakso et al. (2008, 2012), Laban et al. (2018) and Petäjä et al. (2013). Measurements of O₃ concentrations are continuing at the various sites and are referenced in the INDAAF website (<https://indaaf.obs-mip.fr>).



Table 2. Sampling period and concentration data collection efficiency

Ecosystem	Station	Sampling period	Detection limit (ppb)	Data collection efficiency	Season	Measurement altitude (m)
Dry savanna	Ba	2000-2020	0.1	232/248	Dry season: Oct-May Wet season: Jun-Sep	1.5
	Ka	2001-2020		208/240		
	Ag	2005-2018		109/132		
	Bb	2016-2020		47/50		
	Da	2012-2020		87/104		
Wet savanna	La	2001-2020		226/240	Dry season: Nov-Mar	1.5
	Dj	2005-2020		172/186	Wet season: Apr-Oct	
Forest	Zo	2001-2020		208/240	Dry season: Dec-Feb and July-Aug Wet season: Mar-Jun and Sept-Nov	3
	Bo	2001-2020		164/240	Dry season: Dec-Feb Wet season: Mar-Nov	
Agricultural field	Mb	2017-2020		41/43	Dry season: Jun-Oct and Jan-Feb Wet season: Mar-May and Nov-Dec	1.5
Regional savanna/semi-arid	LT	1995-2015	236/248	Dry season: Apr-Sep Wet season: Oct-Mar	1.5	
	Sk	2000-2015	165/192			
	Af	1997-2015	189/221			
	CP	1995-2020	225/248	Dry season: Oct-Mar Wet season: Apr-Sep		

175

2.3 Meteorological parameters and leaf area index

In order to characterize each measurement site, classical meteorological parameters are used such relative humidity, ambient air temperature, rainfall, radiation and leaf area index (LAI). At Ba, Bb, La, Dj and Zo sites, the data on ambient air temperature, relative humidity and rainfall are extracted from the AMMA-CATCH database (Analyse Multidisciplinaire de la Mousson Africaine - Couplage de l'Atmosphère Tropicale et du Cycle Hydrologique; www.amma-catch.org/) and the Observatoire de recherche en environnement "Bassins versants tropicaux expérimentaux" (SO BVET; bvet.obs-mip.fr/) (Ossouhou et al., 2019). The measuring devices used at Ka, La and Bo is described in the same work (Ossouhou et al., 2019). At Bb site, relative humidity, temperature and rainfall are collected in the INDAAF database (<https://indaaf.obs-mip.fr/>). At Da site, measurements of meteorological parameters come from a measuring station installed by the University of Copenhagen (Bigaignon et al., 2020). In Ka, Ag, Bo, Mb, LT, Af, Sk and CP, the meteorological data are provided by the intermediate reanalysis archive (ERA 5) of the European Center for Medium-Range Weather Forecasts (ECMWF). The time series of global solar radiation used in this study at all sites except Dahra are also ERA 5 reanalysis data obtained from ECMWF. LAI data are obtained from MODIS (Moderate Resolution Imaging Spectroradiometer) with a resolution of 0.25 km² for an 8-day time scale centred around each station (Ossouhou et al., 2019). All these parameters are collected at the same sampling period as O₃ concentrations, with the exception of LAI measurements, which began in 2000 (<https://modis.ornl.gov/data.html>).

180

185

190



2.4 NO_x and VOC emissions

The emissions of volatile organic compounds (VOCs) and nitrogen oxides (NO_x) from biomass combustion were downloaded from the ECCAD (Emissions of atmospheric Compounds and Compilation of Ancillary Data) database in the GFED4 inventories for 0.25°x 0.25° grid cells. BVOC emissions are extracted from the MEGAN-MACC inventory in the ECCAD database (eccad.aeris-data.fr). The biogenic NO fluxes used are model outputs in reference to the work of Delon et al. (2010, 2012). They were filtered in the eastern grid from 5° S to 20° N in latitude, and 20° W to 30° E in longitude over the period from 2002 to 2007 and cover only the Ba, Ka, Ag, La, Dj, Zo and Bo sites. ECCAD platform is the emissions database of the international GEIA project (Global Emission Initiative: geiacenter.org) has been developed within the framework of the French atmospheric data center AERIS (<http://www.aeris-data.fr>) (Darras et al., 2022). The GFED4 inventory is based on satellite data of fire activities and vegetation productivity observed since 1997 (eccad.aeris-data.fr). MEGAN (Model of Emissions of Gases and Aerosols from Nature) inventory quantifies net biogenic emissions of isoprene and other gases emitted by vegetation into the atmosphere (Guenther et al., 2006; Sindelarova et al., 2014). Isoprene, α -pinene and β -pinene, which account for the largest proportion of BVOCs emitted by vegetation in Africa (Ferreira et al., 2010; Jaars et al. 2016; Liu et al., 2021; Saxton et al., 2007; Serça et al., 2001), were identified and used in this study. A more detailed description of these emission inventories is discussed in the work of García-Lázaro et al. (2018), Guenther et al. (2006) and Vitolo et al. (2018). For each emission category, NO_x (kg m⁻² s⁻¹) and VOC (kg m⁻² s⁻¹), we use the sum of fluxes from all biomass combustion sources (agricultural, waste combustion, savanna, grassland, scrubland, boreal forest, temperate forest, tropical deforestation, peat degradation and peat fires) at a monthly scale and over the study period for each site.

2.5 Statistical analysis

We use Principal Component Analysis (PCA) and Mann-Kendall test to investigate respectively the different contributions of O₃ precursors from photochemical formation and the monotonic trends in the time series of each site. PCA multivariate analysis method (Jolliffe, 1986), is often used in air quality analyses to identify the major sources of pollutants emitted into the atmosphere (Bruno et al., 2001; Lanz et al., 2007). It specifies the relationships between variables, the phenomena behind these relationships and the similarities between individuals (Mouissi and Alayat, 2016). In this study, the statistical analysis of meteorological data and atmospheric chemical pollutants was carried out on a data matrix made up of ten to eleven variables depending on the site, and 12 individuals representing the months of the year. For PCA implementation, R programming software was used. More detailed information on the calculation of PCA can be found in the literature (Ait-Sahaliaa and Xiu, 2019; Baglama et al., 2021; Duriš et al., 2021; Tsuyuzaki et al., 2020). The Mann-Kendall and seasonal Kendall tests, associated with the calculation of Sen's slope (Sen, 1968) is applied to all sites with at least 10 years of measure using XLSTAT 2022.2.1.1313 software. The trend is said to be statistically significant when the p-value of the test is less than 5%. In the case of Kendall's seasonal test, the seasonal nature of the series is taken into account. The literature provides extensive information on Mann Kendall trends calculations (Frimpong et al., 2022; Hirsch et al., 1982; Kendall, 1975; Merabtene et al., 2016). Another non-parametric breakpoint test (Pettitt test) is carried out using Khronostat 1.01 software to assess possible breaks in homogeneity in the O₃ concentration series and for optimal application of the trend test.

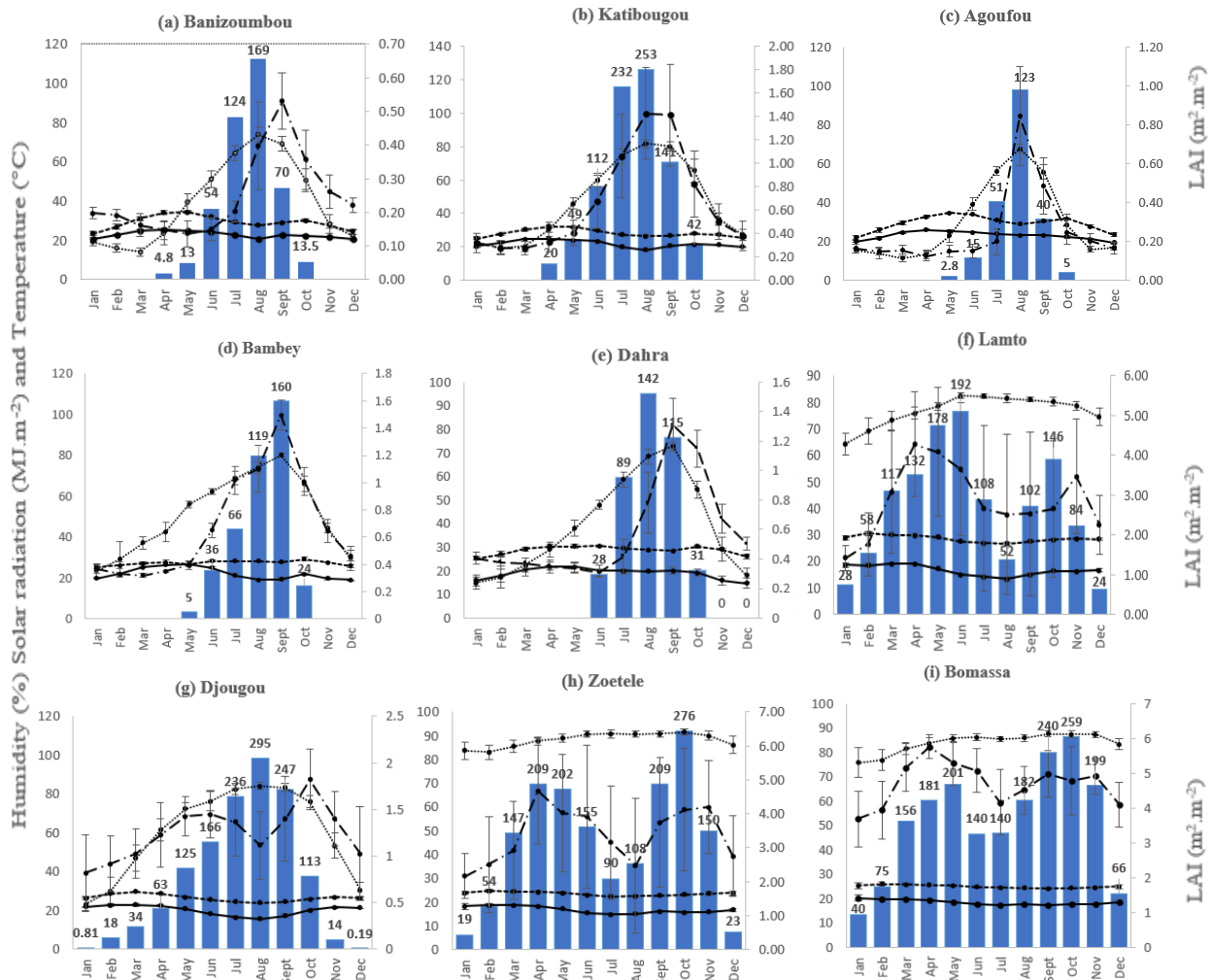
3. Results and discussion

3.1 Meteorological and biophysical parameters variation

The monthly variations of meteorological parameters and leaf area indexes (LAI) are shown in Fig. 2 for all sites. In dry savanna, the rainfall regime is unimodal, with the greatest amounts of rain recorded from July to September corresponding at the maxima of LAI. Mean air temperature ranged from 22.1 ± 0.9°C to 34.9 ± 0.4°C, with air relative humidity from 68% to 82%. The most elevated solar radiation is found at Ag (23.1 ± 0.5 MJ.m⁻²). In wet savanna and forest sites, the rainfall pattern and LAI follow a quasi-bimodal distribution. The mean annual LAI varies from 1.2 ± 0.3 m².m⁻² (Dj) to 4.7 ± 0.7 m².m⁻² (Bo). The most significant monthly variations in relative humidity are found in Dj (23.2 - 84.1%). At Mb site, the maximum rainfall



occurs between March and May, reaching 255 mm in April. The vegetation cover is denser at the end of the first wet season ($1.3 \pm 0.3 \text{ m}^2 \cdot \text{m}^{-2}$ in May) with an average value of humidity around 70%. In Southern Africa, the humidity varies from 13% to 22% year-round except at CP where variations are very low. The maximum of rain is collected between December and January (432 mm on average) at LT, Af and Sk sites and in August at CP (343 mm). LAI maxima are of the order of $1.6 \pm 0.2 \text{ m}^2 \cdot \text{m}^{-2}$ at Af ; $3.1 \pm 0.6 \text{ m}^2 \cdot \text{m}^{-2}$ at LT; $4.0 \pm 0.1 \text{ m}^2 \cdot \text{m}^{-2}$ at CP and $1.7 \pm 0.2 \text{ m}^2 \cdot \text{m}^{-2}$ at Sk in wet season. In wet savanna and forest, the temperature variations are low, as well as in Mb ($23.6 \pm 0.5^\circ\text{C}$). On the other hand, at the South African sites, the temperature reaches amplitudes ranging from 6°C to 10°C . From wet savanna to semi-arid savanna (South Africa), the average solar radiation is below at $22 \text{ MJ} \cdot \text{m}^{-2}$. Along the north-south transect for the study sites, the gradient of humidity, leaf area index and rainfall are positive, whereas it is negative for temperature and radiation.



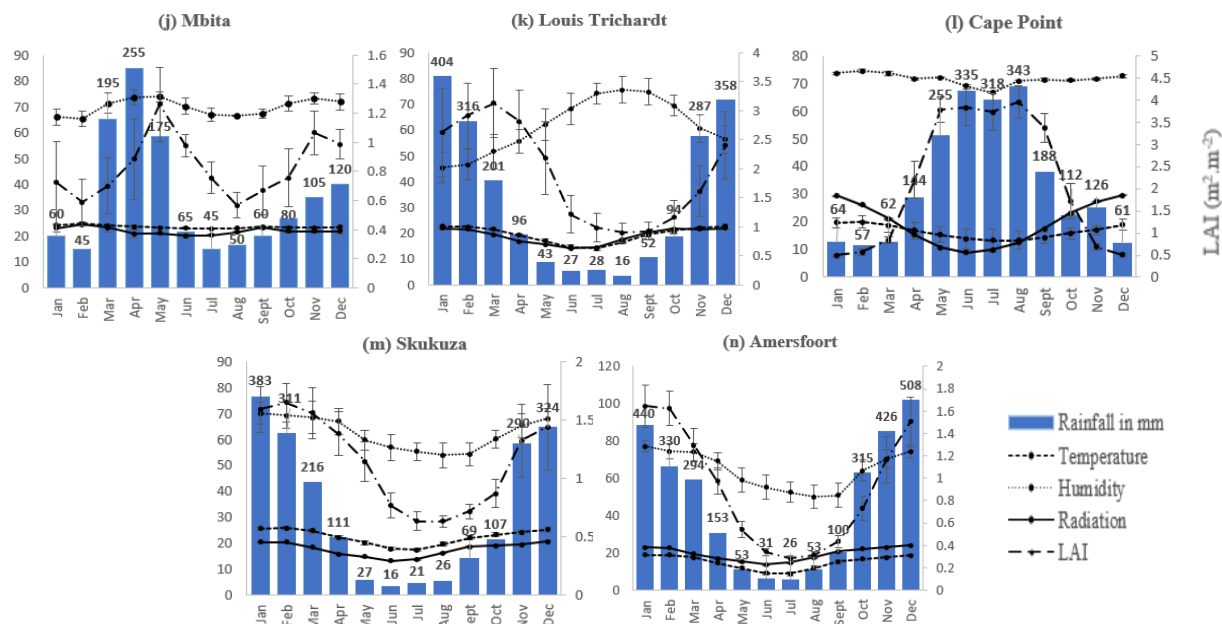


Figure 2. Mean monthly variation in air temperature ($^{\circ}\text{C}$), rainfall (mm), relative humidity (%), solar radiation ($\text{MJ}\cdot\text{m}^{-2}$) and leaf area index ($\text{m}^2\cdot\text{m}^{-2}$). The mean absolute deviation is represented by the vertical bars.

3.2 Characterization of O_3 levels

3.2.1 Seasonal and annual variation in O_3 levels

3.2.1.1 Dry savanna

Figure 3 presents monthly O_3 surface concentrations measured in Ba, Ka, Ag (Fig. 3a), Bb and Da (Fig. 3b) representative of dry savannas in Niger, Mali and Senegal. The seasonal variability of O_3 is well marked: O_3 levels during the wet season are higher than in the dry season (Table 3). On most sites, from January to May, the O_3 concentrations gradually increase to finally reach annual peaks at the start of the wet season (May-June-July). The mean annual cycle of monthly O_3 concentrations at Ba, Ka, Ag (Fig. 4a), Bb and Da (Fig. 4b) are obtained from averages of monthly in situ measurements over the whole studied period. The annual distribution is similar to the regional rainfall pattern. O_3 concentrations decrease as the rainy season progresses, but remain at higher levels compared to the dry season. At dry savanna sites, monthly average surface O_3 concentrations range from 6.1 ± 2.4 ppb to 14.5 ± 2.6 ppb during the dry season, and from 13.9 ± 5.1 ppb to 19.4 ± 3.9 ppb during the rainy season (Table 3). From dry to wet season, O_3 levels increased from 18.7% to 68.5%. The annual O_3 concentrations ranged from 10.5 ± 5.4 ppb at Ka to 14.8 ± 4.3 ppb at Bb (Table 3). The high O_3 concentrations observed at the start of the rainy season are due to soil humidification during this period, which generates biogenic NO emissions pulses in the region. Indeed, the accumulated nitrogen in soils (in the form of ammonium and nitrate ions) from traditional agricultural practices, such as grazing, manure spreading and decomposition of crop residues (Delon et al., 2015; Laville et al., 2005) is released to the atmosphere when the first rains fall on dry soils. Bacterial nitrification is thus activated, leading to nitrogen consumption and consequent release of large pulses of NO (Adon et al. 2010; Delon et al., 2015; Jaegle et al., 2004; Laville et al., 2005; Ludwig et al., 2001; Ossouhou et al., 2019). During the wet season, the decrease in O_3 levels may be attributed to a decrease in NO_x concentrations. Indeed, soil mineral N is used by plants during their root growth phase, and is therefore less available for the production of NO to be released to the atmosphere (Homyak et al., 2014). These observations in dry savanna are confirmed



280

by Stewart et al. (2008) who correlated O₃ production in the Sahel during the wet season with high NO_x concentrations attributed to biogenic emissions during the AMMA (Analyse Multidisciplinaire de la Mousson Africaine) campaign.

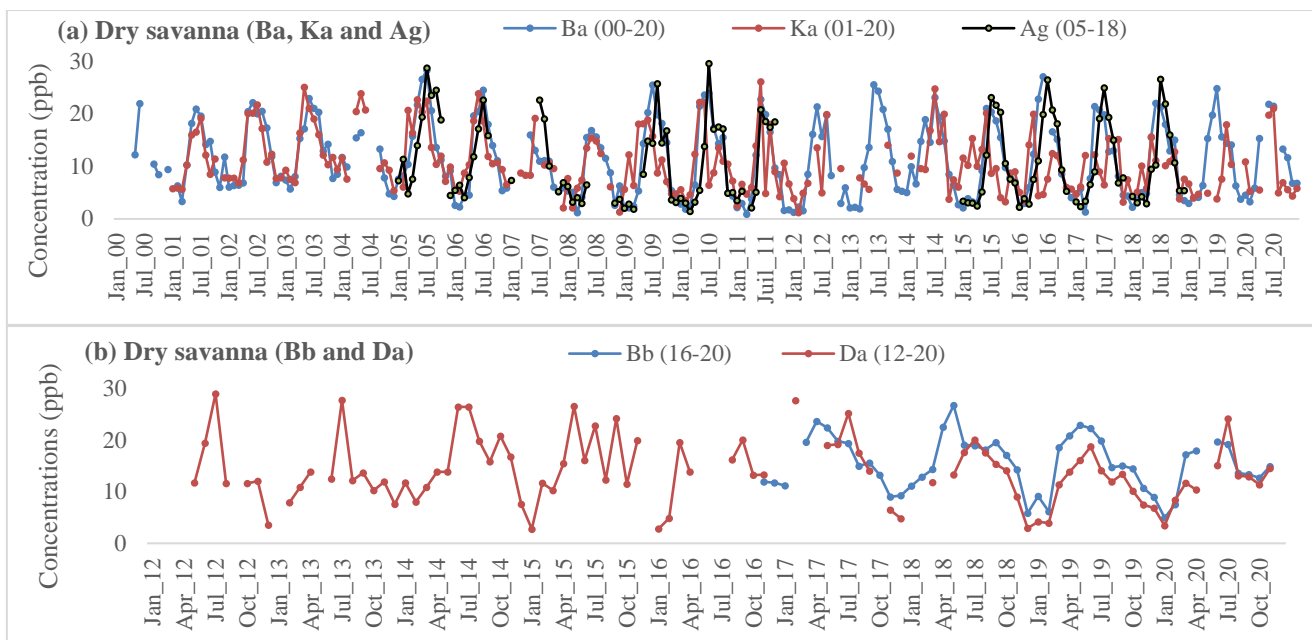
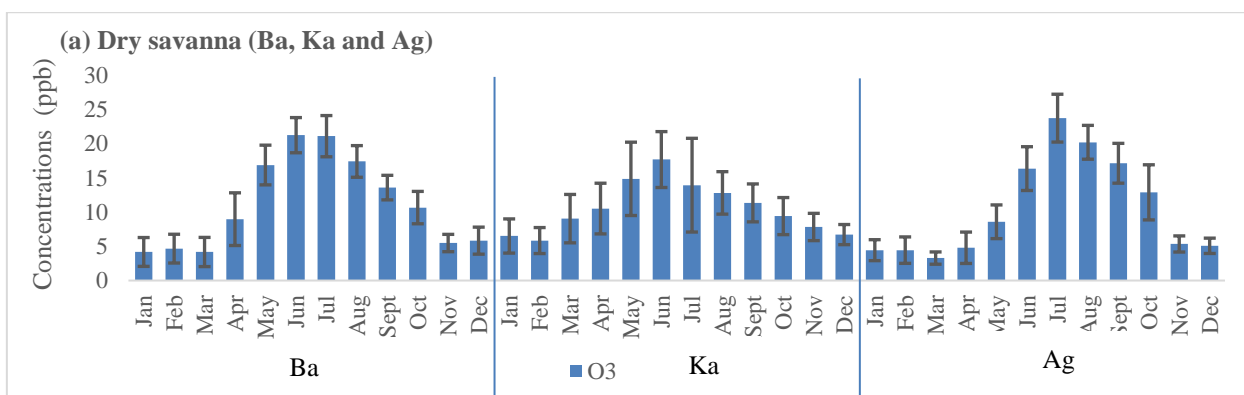


Figure 3. Monthly evolution of O₃ concentrations (ppb) in dry savanna (a) Ba (Niger), Ka, Ag (Mali) and (b) Bb, Da (Senegal).

285



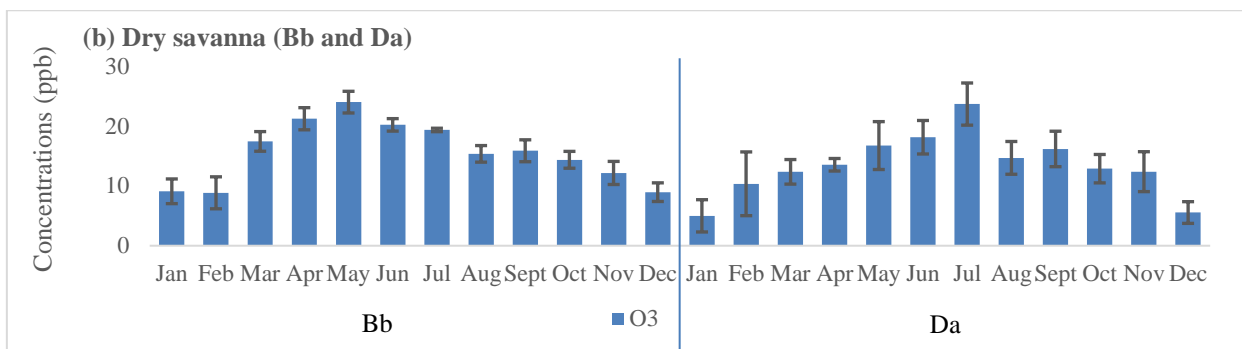


Figure 4. Mean monthly averages of O₃ concentrations (ppb) in dry savanna (a) Ba (Niger), Ka, Ag (Mali) and (b) Ba, Da (Senegal). Bars represent mean absolute deviation.

Table 3. Minimum, maximum and average of monthly, annual and seasonal O₃ concentrations at dry savanna sites (1995-2020)

Ecosystem		Monthly		Annual	Dry season			Wet season		
		min	max	moy	min	max	moy	min	max	moy
Dry savanna	Ba	0.9	28.3	11.2±6.9	4.2±2.7	16.9±3.7	7.6±2.9	13.6±2.5	21.2±3.5	18.3±3.2
	Ka	1.2	26.1	10.5±5.4	5.8±2.6	14.9±6.6	8.8±3.7	11.3±3.8	17.7±5.4	13.9±5.1
	Ag	1.4	29.5	10.5±7.3	3.3±1.1	12.9±4.6	6.1±2.4	16.4±3.8	23.7±4.6	19.4±3.9
	Bb	4.96	26.7	14.8±4.3	8.8±3.5	24.0±2.4	14.5±2.6	15.4±1.9	20.2±1.4	17.7±1.6
	Da	2.8	29.0	13.9±6.3	5.0±3.8	16.7±5.4	11.1±4.0	14.7±3.1	23.7±4.8	18.2±4.0
Wet savanna	La	4.25	20.6	10.8±3.3	9.9±1.4	15.1±2.3	13.5±2.3	6.7±1.1	12.2±1.9	9.0±1.5
	Dj	3.3	24.8	13.5±4.8	10.8±4.5	18.7±2.7	14.1±4.0	9.0±2.0	18.4±2.4	13.2±2.8
Forest	Zo	1.2	11.1	5.2±2.1	7.1±2.1	7.8 ±1.6	7.5±2.1	3.5±1.3	6.6±1.9	4.6±1.6
	Bo	1.5	8.3	3.9±1.1	4.0±1.0	5.2±1.2	4.7±1.4	2.8±1.0	5.4±1.0	3.7±1.0
Semi-agricultural or arid savanna	Mb	10.5	30.2	19.9±4.7	13.8±3.4	25.7±5.7	20.9±4.0	14.1±5.0	22.5±2.7	18.5±3.9
	Sk	6.3	64.1	22.8±7.3	23.0±9.6	30.2±6.0	25.9±7.3	14.5±1.9	29.2±5.6	20.3±5.4
	Af	3.2	55.5	26.9±6.3	19.9±6.2	31.2±7.6	24.5±6.3	23.8±4.9	34.4±7.4	29.0±7.3
	CP	3.3	67.4	26.8±6.2	17.3±5.3	30.4±6.0	23.4±5.6	25.9±6.3	32.1±5.7	29.8±6.1
	LT	9.0	86.6	30.8±8.0	24.7±7.9	40.1±10.8	32.0±8.9	21.3±5.2	36.0±9.1	28.3±8.2

295 **3.2.1.2 Wet savanna and forest**

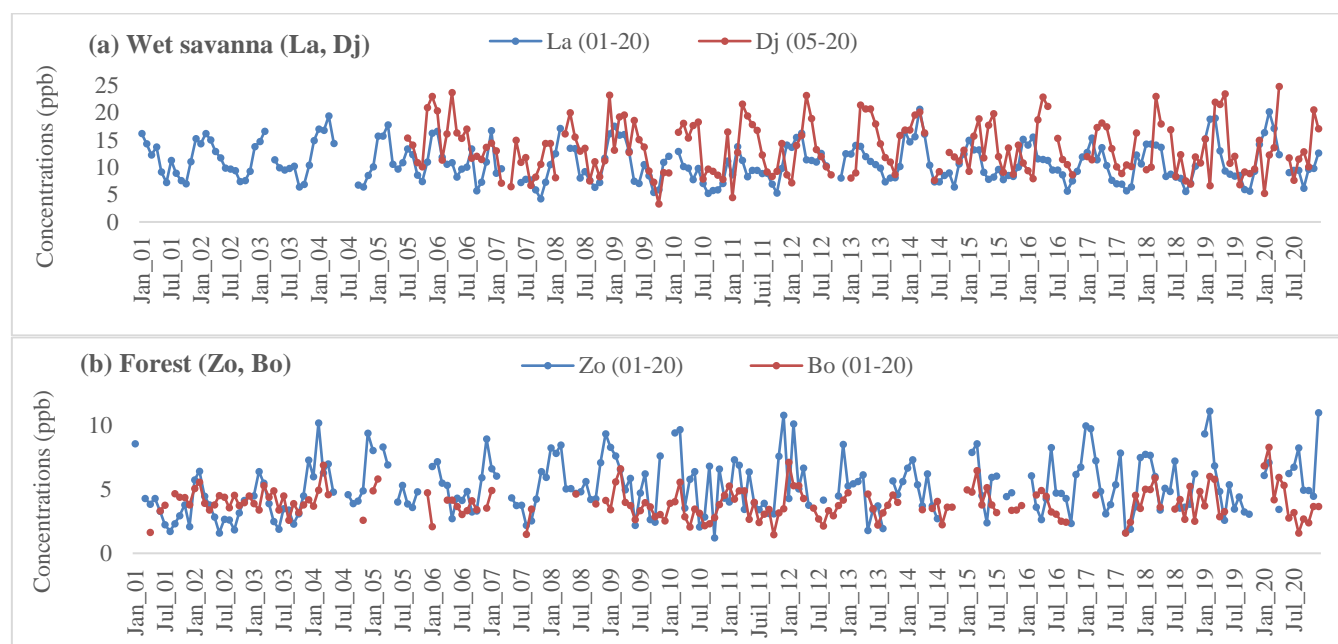
Figure 5 presents the mean monthly surface O₃ concentrations in Dj, La (Fig. 5a), Zo and Bo (Fig. 5b). O₃ concentrations present a seasonality during the year. The maximum of the data series in La is 20.6 ppb in March (dry season) and the minimum is 4.3 ppb in October (wet season). In Dj, the O₃ levels are higher than in La. The monthly highest value recorded in Dj is 24.8 ppb in April (start of the wet season). At the forested ecosystems sites, O₃ concentrations are lower than in dry, wet and semi-agricultural/semi-arid savannas (Table 3). In Zo and Bo, the highest annual peaks are found in February (11.1 ppb and 8.3 ppb respectively). Monthly averages in the dry season ranged from 4.7±1.4 ppb (Bo) to 14.1±4.0 ppb (Dj), and in the wet season from 3.7±1.0 ppb (Bo) to 13.2±2.8 ppb (Dj) (Table 3). The O₃ mean annual cycle is shown in Fig. 6.

300

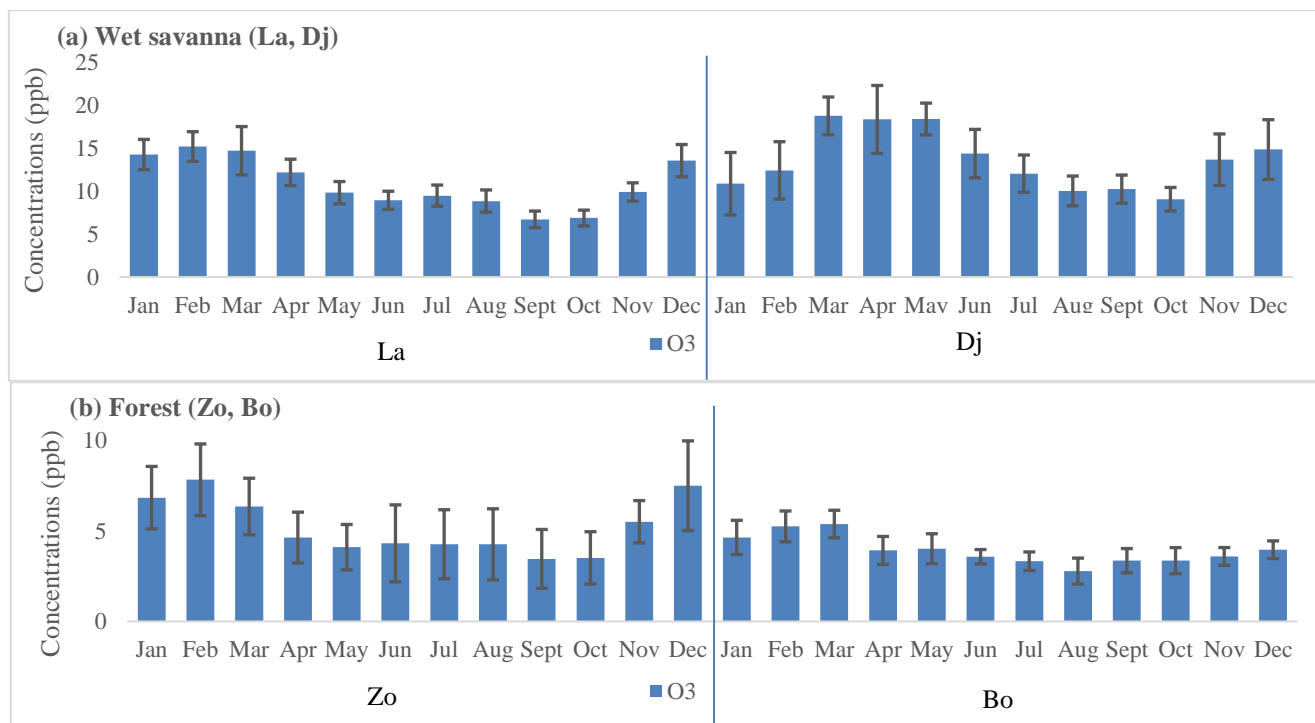
The high O₃ concentrations in dry season in these two ecosystems could be related to the biomass burning source, which is generally recorded during the months of December-February in rural tropical environments. Indeed, Abbadie (2006), Adon et



305 al. (2010) and Galanter et al. (2000) have linked the high O₃ concentrations recorded in the dry season to the presence of NO_x emitted by biomass combustion in the wet savanna. According to Adon et al. (2010), Baldy et al. (1996), Clain et al. (2009), Cros et al. (1992), Hamdun and Arakaki (2015), Martins et al. (2007), Oluleye et al. (2013) the biomass burning is likely to contribute significantly to O₃ production through precursor emissions (NO_x and CO) in the dry season (wet savanna) with nearly 30% to 80% of the savanna ground surface burnt annually between December and February. In other forests such as in
 310 Nepal, Kiros et al. (2016) also attribute high O₃ concentrations to increased burning of agricultural residues and forest fires. The high O₃ concentrations measured in Tranquebar (India) have been linked to increased emissions of NO_x and other precursors from various sources (Debaje et al., 2003). Compared to wet and dry savannas, forest sites recorded the lowest O₃ amounts due to significant dry deposition of O₃ on the ground, on foliage and trees (Mari et al., 2011; Rummel et al., 2007; Saunois et al., 2009). Tropical forests are shown to be important O₃ sinks. A strong gradient of O₃ between forest and dry
 315 savanna in West Africa has been observed from aircraft measurements (Saunois et al., 2009).



320 **Figure 5.** Monthly evolution of O₃ concentrations (ppb) in (a) humid savanna, La (Cote d'Ivoire) and Dj (Benin) and (b) in forest, Zo (Cameroon) and Bo (Congo).



325 **Figure 6.** Mean monthly averages of O₃ concentrations (ppb) a) in humid savanna, La (Cote d'Ivoire) and Dj (Benin) and b) in forest, Zo (Cameroon) and Bo (Congo). Bars represent mean absolute deviation.

3.2.1.3 Agricultural and semi-arid savanna

330 Figures 7 presents the monthly evolution of surface O₃ concentration in agricultural site (Mb) and semi-arid savanna sites (LT, CP, Sk and Af). At Mb site, monthly O₃ concentrations do not exceed 30.2 ppb (Table 3). At the CP, LT, Sk and Af sites, O₃ levels are almost twice as high as in West African sites. The mean annual cycle of O₃ concentrations (Fig. 8a and b) shows that at Mb, O₃ levels are almost similar between seasons (Table 3). In southern African ecosystems, dry-season O₃ concentrations are the highest at LT and Sk. The annual averages are around 19.9±4.7 ppb at Mb; 22.8±7.3 ppb at Sk; 26.9±6.3ppb at Af; 26.8±6.2ppb at CP and 30.8±8.0ppb at LT (Table 3).

335 The O₃ levels observed in Mb during the dry season could be associated with biomass burning. Based on the analysis of burned surface areas, Bakayoko et al. (2021) indicated that Mb is strongly influenced by biomass burning from northern and southern sides during both dry seasons. High O₃ levels measured at Mb site during the dry season show similar values as in Nairobi, Kenya, during the same months (Kimayu et al., 2017). At southern African sites, O₃ levels could be attributed to a combination of regional and local influences, including emissions from industrial, vehicular and domestic biomass combustion to biomass combustion events in sub-Saharan Africa (Mozambique, Zambia, Zimbabwe and Angola) recirculated by anticyclonic air mass processes (Baldy et al., 1996; Laban et al., 2018; Martins et al., 2007; Swap et al., 2003; Tiitta et al., 2014). Biomass combustion is considered as a major source of O₃ precursors in South Africa (Ngoasheng et al., 2021; Vakkari et al., 2013) and in Southern Africa (Heue et al., 2016) and may explain the O₃ levels observed in dry season at LT and Sk. High O₃ levels in the wet season are thought to be due to soil microbial activity (Swartz et al., 2020a) as well as long-range transport of air pollutants emitted from the industrialized Highveld region (Abiodun et al., 2014; Ojumu, 2013). During the austral winter, O₃ concentrations in the boundary layer are higher (e.g. at CP and Af) due to a systematic increase in O₃ precursors from households, combustion for space heating (Bencherif et al., 2020; Laban et al., 2018; Lourens et al., 2011; Oltmans et al.,



350

2013; Swartz et al., 2020b). The high concentrations measured at Af could also be due to industrial activities located near this site (Lourens et al., 2011).

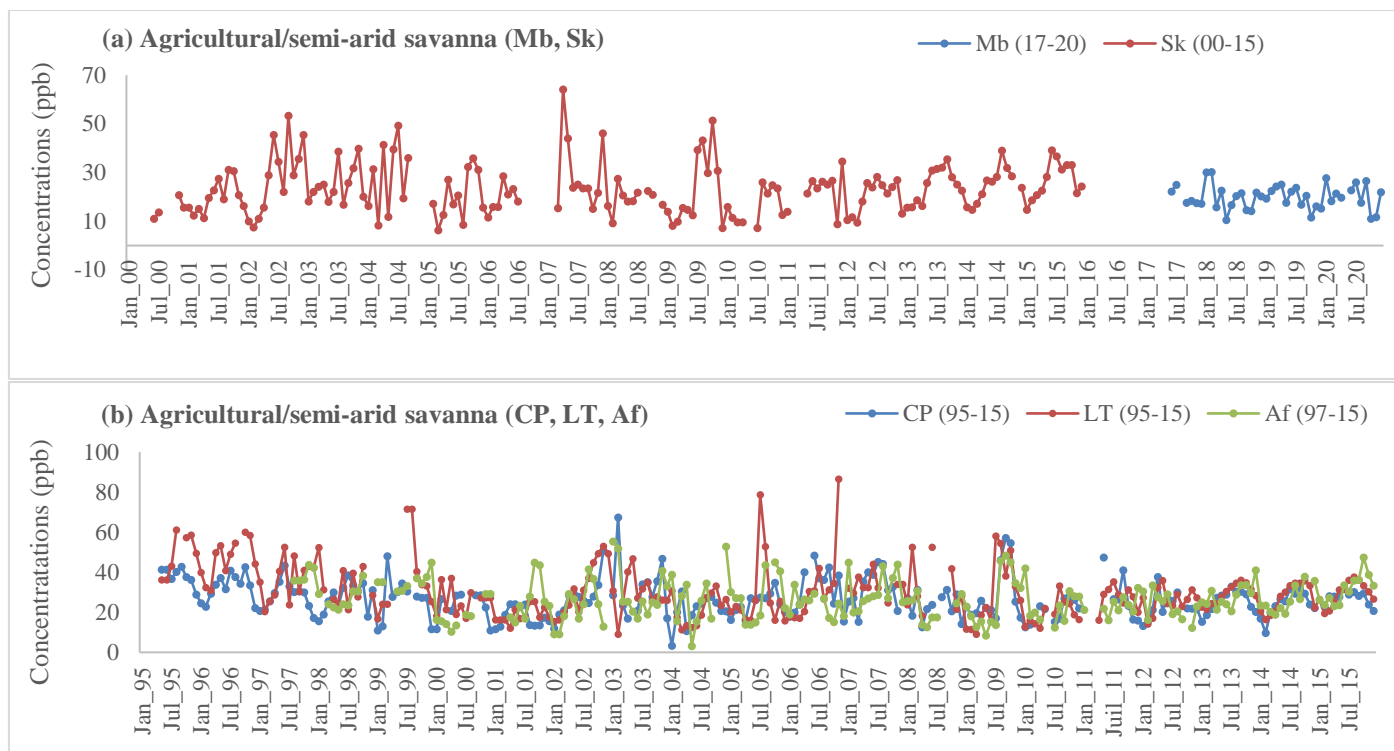
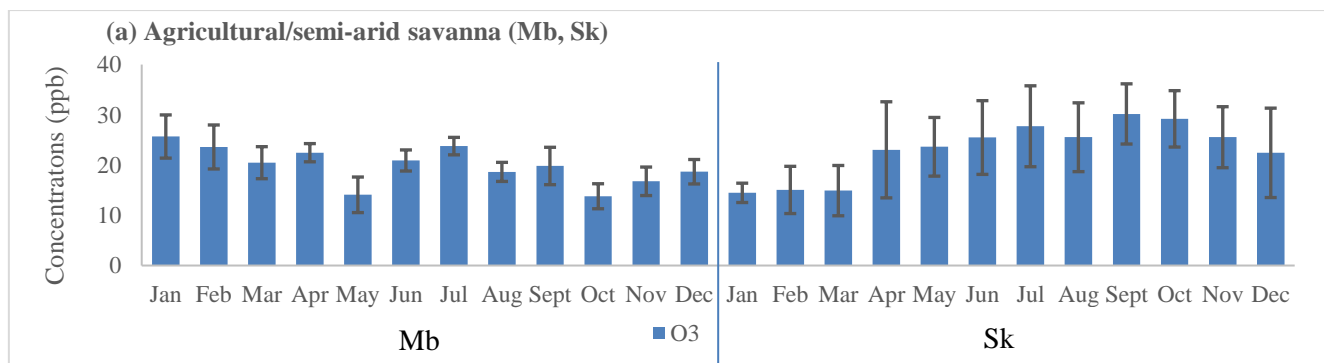
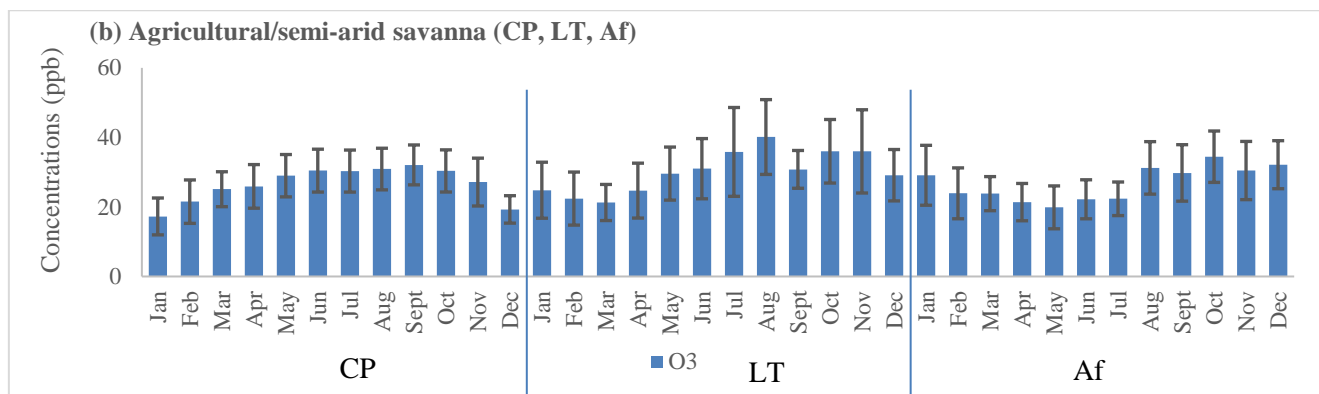


Figure 7. Monthly evolution of O₃ concentrations (ppb) in Agricultural/semi-arid savanna (a) Mb (Kenya) and Sk (South Africa) and (b) CP LT and Af (South Africa).





360 **Figure 8.** Mean monthly averages of O₃ concentrations (ppb) in Agricultural/semi-arid savanna (a) Mb (Kenya) and Sk (South Africa) and (b) CP, LT and Af (South Africa). Bars represent mean absolute deviation.

3.2.2 O₃ levels in Africa, set in a global context

O₃ concentrations measured at the 14 studied site are mapped on a seasonal and annual scale (Fig. 9).

365

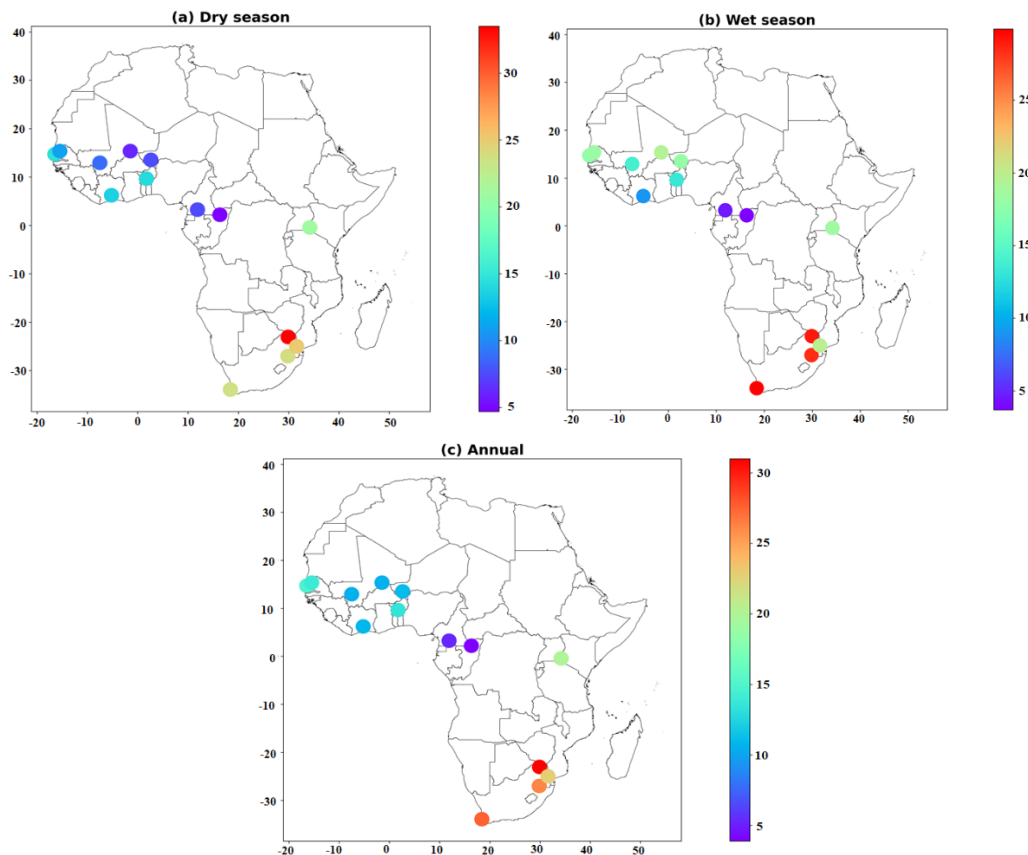


Figure 9. Seasonal and annual mapping of O₃ concentration levels in (a) Dry season, (b) Wet season and (c) Annual over the 14 studied sites.



370

We compared African ozone levels related in this study with studies carried out in Africa and around the world over the last 20 years (Table 4, Fig. 10). The bibliographical synthesis takes into account studies where data measurement methodology has been clearly described. Sites where concentrations have been measured by passive samplers are listed. We have identified among others, sites in Nepal, North America, North-Eastern Europe, Asia and Africa. Figure 10 focuses more on O₃ monitoring studies in Africa.

375

Table 4. O₃ concentrations at various sites worldwide as reported in literature

Sites	Type	Period	O ₃ (ppb)	References
India, Tranquebar	Rural	May 1997 -Oct 2000	17±7 - 23 ± 9	Debaje et al. (2003)
Sweden, Malmö (20 sites)	Rural	(16–24 Apr 2012 ; 28 May–4 Jun; 20–27 Aug 2012	37.0±5.4	Hagenbjörk et al. 2017
	Urban		35.0±3.9	
	Traffic		33.6±3.5	
Sweden, Umeå (20 sites)	Rural		27.7±8.4	
	Urban		26.7±7.3	
	Traffic		25.2±6.9	
China, Waliguan mountain	Rural	Sept 99-May 2001	44.9	Carmichael et al. 2003
Taiwan, Shui-Li	Rural		25.0	
Malaysia, Tanah Rata	Rural		16.0	
Indonesia, Bukit Kototabang	Rural		10.7	
Inde, Agra	Rural		30.8	
Argentina, Isla Redonda	Rural		15.9	
Brazil, Arembepe	Rural		19.2	
Turkey, Camkoru	Rural		35.4	
Arab Emirates, Al-Ain	Rural		Apr 2005-Apr 2006	
	Industrial	5.9		
	Traffic	4.4		
	Commercial	5.9		
	Residential	7.3		
American Samoa Island, Tutuila	Urban and Rural	1990-2015	13.7 ± 1.0	Lu et al. 2018
Chili, El Tololo			32.0 ± 1.3	
South Africa, Cape point			24.3 ± 1.1	
Australia, Cape grim			24.9 ± 0.8	
New Zealand, Baring head			21.4 ± 1.6	
Syowa			25.2 ± 0.9	
Neumayer-G			24.3 ± 1.5	
Arrival heights			25.9 ± 1.5	
South Pole			28.4 ± 1.7	
Nepal, Bode			Urban	
Nepal, Indrachowk	37.9 ± 6.2			
Nepal, Maharajgunj	46.4 ± 12.0			
Nepal, Mangal Bazaar	40.3 ± 8.0			
Nepal, Suryabinayak	41.3 ± 5.4			
Nepal, Bhaisepati	47.7 ± 9.1			
Nepal, Budhanilkantha	Suburban	50.3 ± 11.3		



Nepal, Kirtipur	Rural	23 March -18 May 2013	46.9 ± 9.8	Kiros et al. 2016
Nepal, Lubhu			50.7 ± 8.6	
Nepal, Bhimdhunga			59.7 ± 11.9	
Nepal, Nagarkot			70.1 ± 9.7	
Nepal, Naikhandi			53.5 ± 13.0	
Nepal, Nala Pass			43.6 ± 10.5	
Nepal, Sankhu			57.6 ± 11.9	
Nepal, Tinpiple			54.4 ± 13.4	
Barrow Atmospheric Baseline Observatory	Remote site	1973-2015	15-44	Cooper et al. 2020
Mauna Loa Observatory (MLO)	Remote site	1973-2015	26-65	
American Samoa Observatory	Remote site	1973-2015	5-20	
South Pole Observatory	Remote site	1973-2015	17-40	
China	Rural site	2014-2017	34	Dufour et al. 2021
Central East China			36	
Beijing–Tianjin–Hebei region			39	
Yangtze River Delta			35	
Pearl River Delta			31	
North America, Europa and Est Asia (Korea et Japan)	3136 Rural sites	2010-2014	0-56 and more	Gaudel et al. 2018
North America, Europa and Est Asia	3348 Rural sites and 1453 urban sites	2010-2014	0-100 and more	Fleming et al. 2018
North America, Europa and Est Asia	Rural site	1996-2005	15-55	Young et al. 2018
North America, Europa and Est Asia	Rural and urban site	2010-2014	10-60	Schultz et al. 2017
Eastern North America	Rural site	2000-2014	26-38	Chang et al. 2017
	Urban site		28-38	

380 Several sites reported in Table 4 and Fig. 10 are exposed to high O₃ concentrations. These different levels observed in Africa
and around the world are in most cases above values displayed in this study, with the exception of sites in southern Africa.
The main reason for the discrepancies could be the proximity of these sites to O₃ precursor sources. They are generally located
close to industrial, commercial and residential areas, not far from road traffic, garbage dumps, etc., where precursor emissions
are high. Some sites may also be influenced by continental air masses containing gaseous pollutants. At urban sites such as
385 Al-Ain, Bamako, Dakar, Abidjan and Cotonou, the low O₃ levels are due to the saturated NO_x regime observed at these sites,
which limits photochemical O₃ production (Adon et al., 2013; Bahino et al., 2018; Salem et al., 2009). At INDAAF sites,
concentrations are lower because of their rural characteristics, generally far from anthropogenic sources, and much more
influenced by biogenic activities from soils and vegetation. Results are fairly illustrative of the various mitigation or vigilance
measures that need to be adopted to ensure the environmental well-being of each ecosystem. The additional efforts must
390 therefore be made, through projects or programs, to densify monitoring networks for polluting gases in general and O₃ in
particular, especially in Africa, where very few long-term monitoring exist.

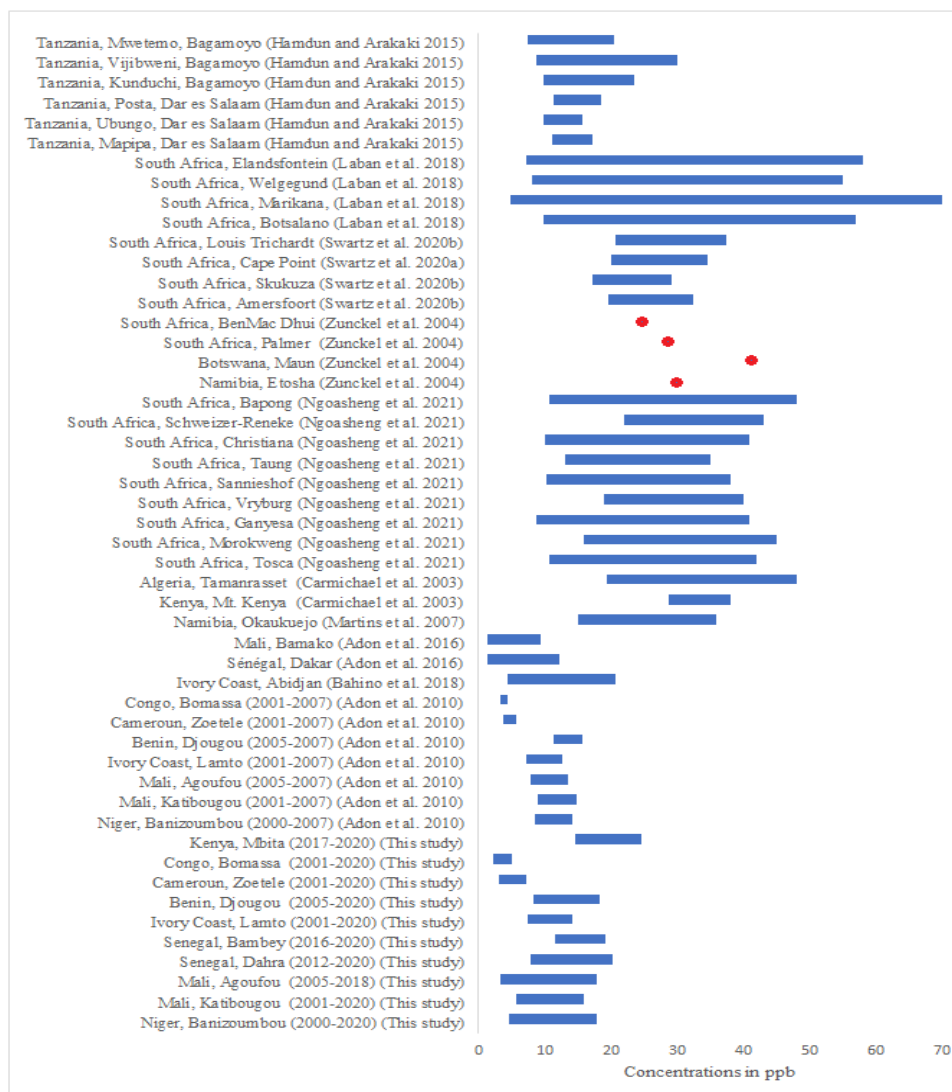


Figure 10. Overview of O₃ monitoring studies in Africa. Blue bars represent lower and upper range of means if reported. Red points represent average concentration of O₃.

395

3.3 Monthly variation in NO_x and VOC anthropogenic and natural emissions

Tropospheric O₃ concentrations result from atmospheric chemistry involving precursors especially NO_x and VOCs, and from transport (distance and time). Locating the sources of precursors (both biogenic and anthropogenic), and their amplitude, is therefore necessary to explain O₃ levels, on a local and regional scale.

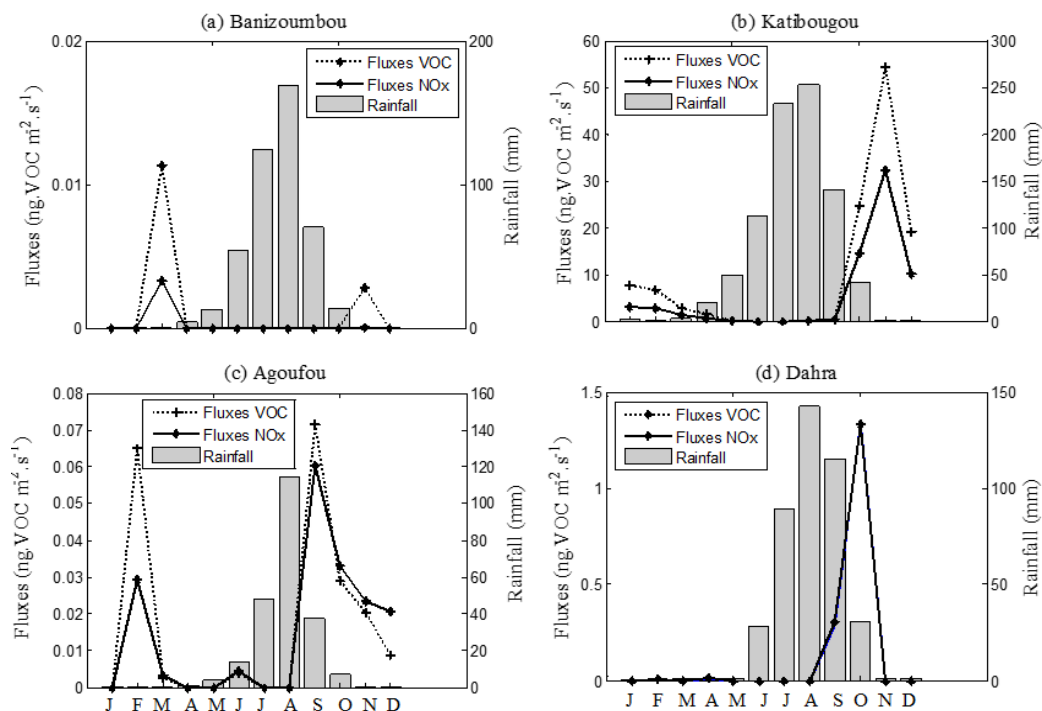
400

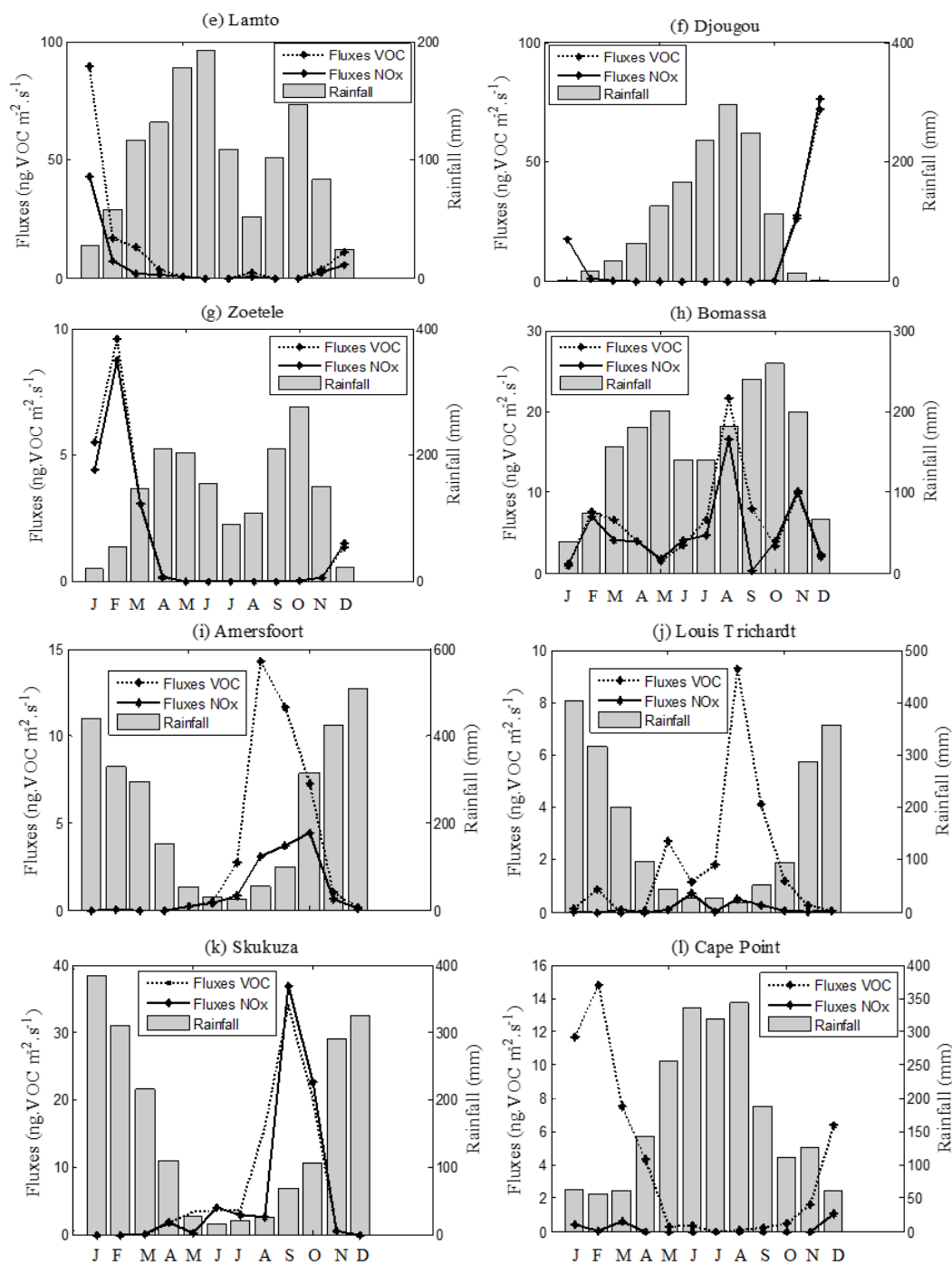
3.3.1 NO_x and VOC anthropogenic emissions

Monthly variation in anthropogenic NO_x and VOC emissions are studied at all sites, with the exception of the Bb station, where emission data are not available (Fig. 11). In dry savanna, during the wet season, NO_x and VOC fluxes are very low. On the other hand, maxima are observed in the dry season with the highest emissions found in Ka. Indeed, the monthly averaged



405 biomass combustion emissions (GFED4) over the 18-year period (1998-2015) in the Sahel show that Ka is significantly
 affected by the biomass combustion source in November (Ossouhou et al., 2019). In wet savannas (La, Dj), and forest (Zo),
 NO_x and VOC fluxes reach their maxima during the dry season. The mean flux estimates are respectively 14.5; 24.2; 4.9
 ng.m⁻².s⁻¹ for NO_x and 26.8; 29.4; 5.5 ng.m⁻².s⁻¹ for anthropogenic VOCs at La, Dj and Zo. High dry-season NO_x emission
 rates observed are linked to biomass combustion sources (Abbadie, 2006; Adon et al., 2010; Akpo et al., 2015; Ossouhou et al.,
 410 2019; Swartz et al., 2020b). In Bo, high NO_x and VOC fluxes are observed in the wet season, unlike in Zo, corroborated by
 Ossouhou et al (2019) over the period 1998-2015. The source of these recorded anthropogenic emissions could be biomass
 combustion. Indeed, according to the work of Sauvage et al. (2005), the period from August to September corresponds to a
 peak in biomass burning activity in the southern African countries (Mozambique, Zimbabwe, South Africa). Moving air masses
 over Central Africa via the northern edge of the continental anticyclone could explain such high emissions at Bo in August-
 415 September. NO_x and VOC fluxes are quantifiable in February (dry season) at Mbita and are thought to be due to the combustion
 of biomass from agricultural activities and from biomass burning in savannas north of the site (South Sudan, Central African
 Republic and Democratic Republic of Congo) (Bakayoko et al., 2021; Boiyto et al., 2017b). At the South African sites, the
 mean fluxes vary from 0.3 ng.m⁻².s⁻¹ (LT) to 10.2 ng.m⁻².s⁻¹ (Sk) for NO_x and from 2.9 ng.m⁻².s⁻¹ to 11.8 ng.m⁻².s⁻¹ (Sk) for
 VOCs with the maxima recorded in dry season. These values may be explained by significant anthropogenic emissions from
 420 domestic biomass burning and solid fuel combustion resulting in high levels of pollutants in South Africa's Highveld region
 (Kai et al., 2022). By developing an African regional inventory of anthropogenic emissions (wood and charcoal burning,
 charcoal manufacture, open waste burning etc.), Keita et al. (2021) estimate that Southern Africa is among the highest emitting
 regions for NO_x, due to industrial sources and power plants. Using satellite data for NO₂ between 2005 and 2017, Oluleye
 (2021) has noted that nitrogen dioxide concentrations during the dry season were up to 200% higher than the values observed
 425 during the rainy season. The high NO_x and VOC levels observed at the different sites during the dry season result from these
 different sources, releasing large quantities of precursors in the atmosphere, and not washed out by rainfall.





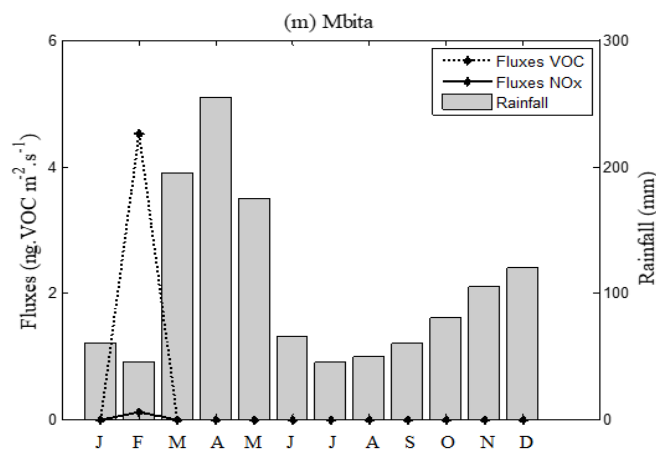


Figure 11. Mean monthly fluxes of NOx and VOC from biomass combustion estimated by the GFED4 inventory for 0.25° x 0.25° grid cells centered on each of dry savanna, wet savanna, forest and semi-Agricultural/arid savanna sites.

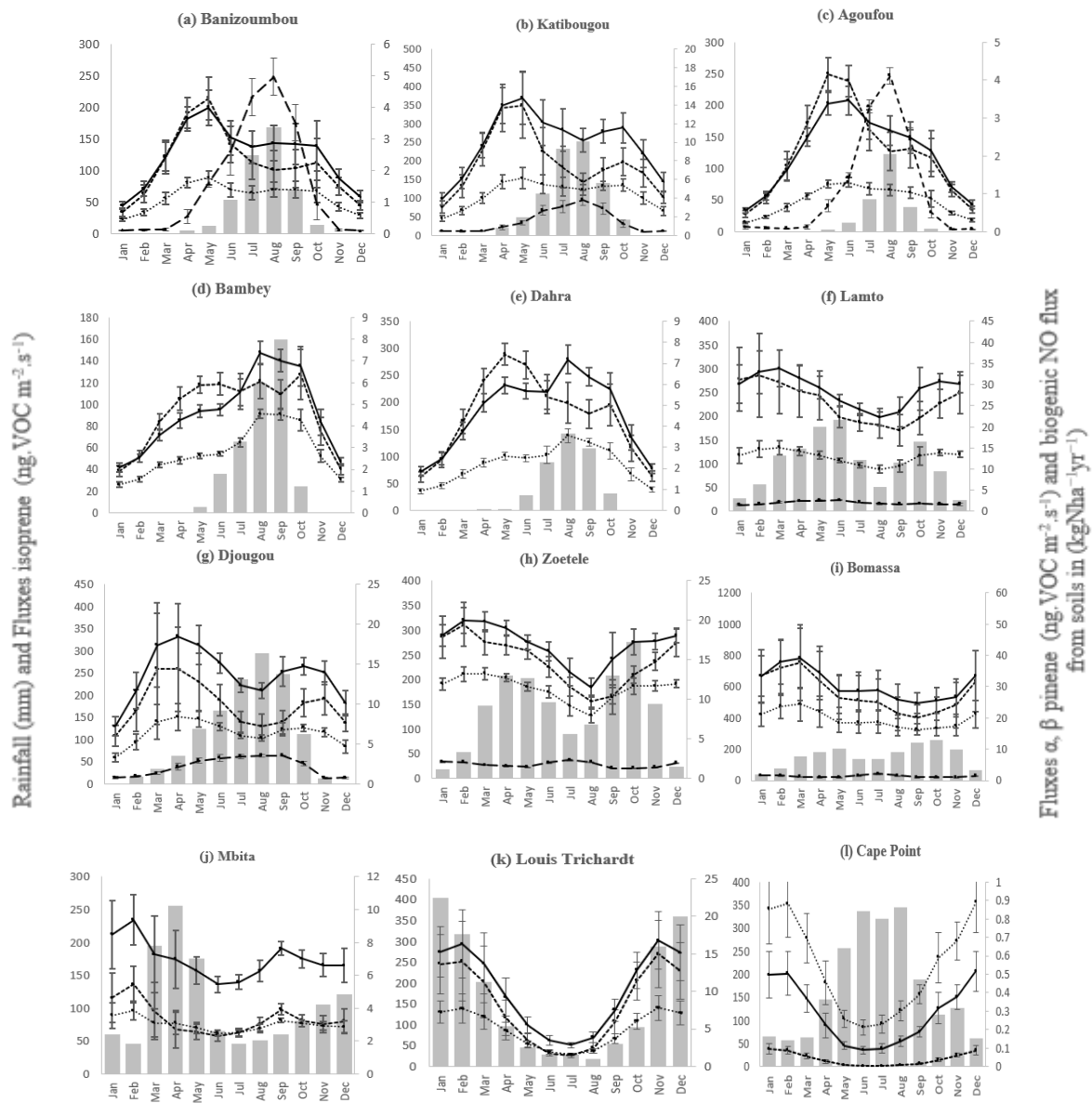
435 3.3.2 NOx and VOC natural emissions

Monthly variations in VOCs (α pinene, β pinene and isoprene) and biogenic NO around the studied sites are shown in Fig. 12. Biogenic NO fluxes in dry savanna show a bell-shaped variation, peaking in August (wet season). In wet savanna and forest, the highest values are also recorded during the wet season. Peaks range from 2.1 ± 0.1 (Bo) to 5.0 ± 0.6 kgNha⁻¹.year⁻¹ (Ba) in the three ecosystems. These peaks of emission could be explained by the correlation between soil moisture, NO production in the soil and its release to the atmosphere, as shown in Delon et al., (2010), Galy-Lacaux et al., (2009), Onojeghuo et al. (2017) and as illustrated in Sect. 3.2.1.1. The soil moisture content during the dry season is higher in wet savanna and forest than in dry savanna, which limits the NO pulse in these ecosystems (Delon et al., 2012). Monthly profile of BVOC fluxes (isoprene, α pinene and β pinene) in dry savanna shows a maximum at the end of the dry season/beginning of wet season at Ba, Ka and Ag, or during the wet season at Bb and Da. Isoprene fluxes are more obvious at Da (214.2 ± 30) ng.m⁻².s⁻¹ whereas α pinene, and β pinene exhibit larger values at Ka site (11.2 ± 1.8 ; 5.2 ± 0.8 ng.m⁻².s⁻¹ respectively). In La, Dj, Zo, Bo and Mb, BVOC maxima fluxes are also obtained at the end of the dry season/beginning of the wet season. A drop in these fluxes is then observed during the wet season. From dry savanna to forest, the transect gradient is positive for BVOC emissions, and is due to the abundance of vegetation in wet savanna (La) and forest. At Southern African sites, more specifically LT, Af and Sk, the highest values of BVOC are reached in the wet season: 189.6 ± 46.8 ng.m⁻².s⁻¹ (isoprene), 14.2 ± 2.7 ng.m⁻².s⁻¹ (α pinene) and 5.6 ± 1.0 ng.m⁻².s⁻¹ (β pinene). At CP, the maximum emissions are measured in the dry months of January/February. BVOC emission rates variation is a function of several factors, namely temperature, sunshine (Guenther et al., 1993), carbon dioxide (CO₂) concentration, precipitation, plant species (Jaars et al., 2016), crops, shrubs (Guenther et al., 1995), modulated on seasonal and interannual time scales by changes in land cover and canopy environment (Chen et al., 2018) as well as by climate change. In dry savanna, the peaks in BVOC observed at the end of the dry season (April/May) could therefore be due to strong radiation and high temperatures which could impact certain woody species (Zwarts et al., 2023), and cause biogenic emissions (Saxton et al., 2007). Indeed, woody species in grasslands are major sources of BVOC emissions (Jaars et al., 2016). Furthermore, positive correlations were obtained between isoprene emissions and air temperature (Jaars et al., 2016; Guenther et al., 1993; Saxton et al., 2007). In the forest, Serça et al. (2001) reported that the average ambient isoprene concentration for a tropical forest in northern Congo was the highest at the start of the rainy season and fell sharply at the end of the rainy season. At the Welgegund site (South Africa), which belongs to the same ecosystem as LT, Af and Sk, Jaars et al. (2016) also measured the highest BVOC concentrations during the rainy season as in this study, and increased BVOC concentrations were associated with high soil moisture. Gradual decrease in BVOC fluxes during the wet season observed at most of the sites is thought to be



due to the uptake of VOCs by soils, thanks to the microbial activity that develops during this period. Soils could therefore play an important role as isoprene sinks (Gray et al., 2015).

465



470

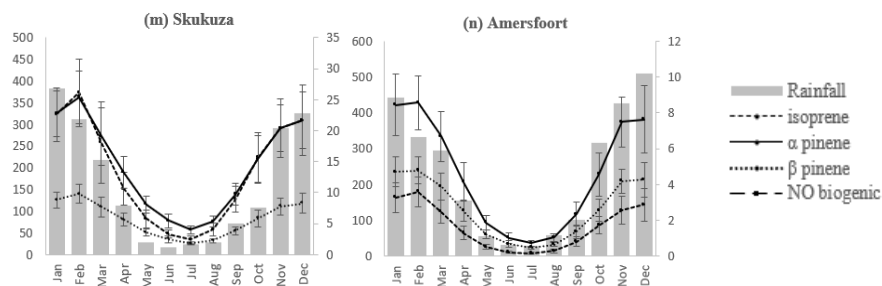


Figure 12. Mean monthly fluxes of BVOCs estimated by the MEGAN inventory for $0.25^\circ \times 0.25^\circ$ centered meshes and biogenic NO in dry savanna, wet savanna, forest and semi-Agricultural/arid savanna.

475 **3.4. Contributions of meteorological variables, NO_x and VOC to O₃ production**

In this section, we use PCA to estimate the relevant number of axes (Sect. 3.4.1) to identify the major sources of O₃ precursor emissions at each site, based on their contribution to the construction of the axis and the quality of their representation on the axis (Sect. 3.4.2).

480 **3.4.1. Estimation of the inertia of the studied factors**

At all sites, ten to eleven factors (meteorological variables and chemical pollutants) are studied. Each factor could correspond to a given axis. However, the cumulative inertia calculated indicated that the first two axes ranged from 79.9% (Ag) to 95.4% (Af) at all sites (Fig. 13). These values are well above the reference value of 54.2% (Tsuyuzaki et al., 2020). These axes therefore represent the main axes. The high inertia values obtained indicate that the factors studied are not independent and that there are strong links between them. The projection of the dataset onto the factorial plane (with two axes) is therefore a good approximation of the air quality at each site, as it contains most of the available information.

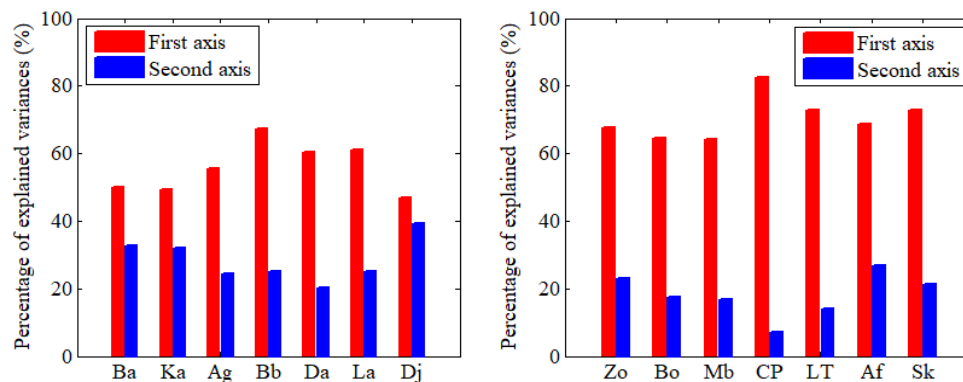


Figure 13. Decomposition of the total inertia of O₃ precursors on the factorial axes.

490 **3.4.2. Characterisation of O₃ precursor emission sources and studies of correlations**

3.4.2.1 Dry savanna

At the dry savanna sites, two groups of pollutants can be identified through their contribution to the two axes. O₃, α pinene, β pinene, isoprene and NO are strongly correlated with the first axis ($0.58 < r^2 < 0.98$) and NO_x, VOCs anthropogenic fluxes correlate well with the second axis ($0.62 < r^2 < 0.92$). These results suggest the presence of two major sources of precursors: biogenic and anthropogenic activities. Calculating the Pearson correlation between the different pollutants, we observe a good

495



dependence of O₃ only with all biogenic precursors ($0.51 < r < 0.95$) at Ba, Ka and Ag in the presence of high relative humidity and precipitation ($0.64 < r < 0.95$) (Table 5). On the other hand, at Bb and Da, isoprene correlates well with O₃ ($r = 0.79$). It appears as a dominant precursor under the influence of temperature and radiation, which are also well correlated with O₃ ($0.5 < r < 0.76$) (Table 5). The main contributions to the formation of the first axis are observed for BVOC (39.5% to 44.6%) with a good quality of representation (0.5 to 0.9) (Fig. 14). The contribution of biogenic NO is about 10%. The most relevant meteorological variables (humidity, temperature, precipitation, radiation) contribute significantly, ranging from 10.5% to 30.8%. In dry savanna, Oluleye et al. (2013) estimated that rain was responsible for 62% of the O₃ distribution in the West African region, excluding the precursors NO, CO and hydrocarbons, as also illustrated in our results. Saunois et al. (2009) have shown that soil NO_x emissions, combined with the northward advection of volatile organic compounds (VOCs), play a key role in O₃ production in dry savanna regions. This large-scale impact of biogenic emissions has also been verified by Williams et al. (2009), who estimate that 2-45% of tropospheric O₃ over equatorial Africa may originate from NO_x emissions from African soils. All these works are in agreement with the results of this study.

3.4.2.2 Wet savanna and forest

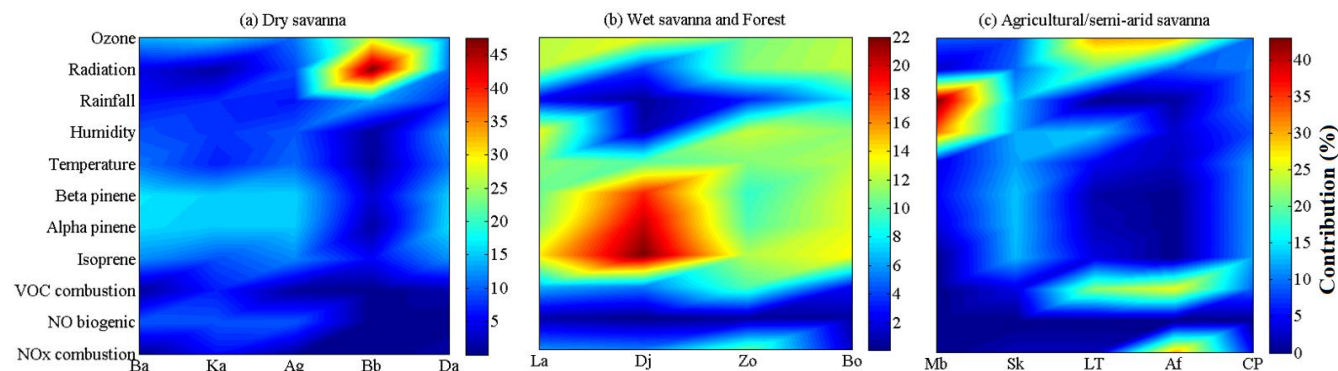
In wet savanna and forest, pollutants such as O₃, α pinene, β pinene, isoprene, anthropogenic NO_x and VOCs (except at Bo and Dj) are positively correlated to the same axis ($0.62 < r^2 < 0.97$), while only NO is linked to the second axis. The major sources highlighted in this case could be anthropogenic activities and those linked to biogenic vegetation on the one hand, and biogenic soil activities on the other. Strong Pearson correlations are observed between O₃, NO_x and the VOCs ($0.49 < r < 0.92$) (Table 5). Temperature and radiation are also well correlated with O₃ ($0.54 < r < 0.89$) in these two ecosystems. The dominant contributors are then BVOC (31% to 60.8%), temperature (11% to 12.1%), radiation (11.1% to 12.4%) (Fig. 14). Anthropogenic emissions at La and Zo make a significant contribution (5.8% to 10.2%). These results are corroborated by the literature. Indeed, radiation and humidity facilitate the propagation of radical chain reactions and the production of hydroxyl radicals (OH) at these sites (Graedel and Crutzen, 1993). According to several authors, O₃ levels tend to increase under warm, sunny conditions favorable to photochemical O₃ production (Hamdun and Arakaki, 2015; Morakinyo et al., 2020). Moreover, Aghedo et al. (2007), Mari et al. (2011), Saunois et al. (2009) and Saxton et al. (2007) have reported that vegetated areas emit large quantities of biogenic organic compounds that influence O₃ production in the presence of light and temperature.

3.4.2.3 Agricultural and semi-arid savanna

At the South African sites, the major sources of pollutant vary from one site to another. At Af, we identify a first group of pollutants (α pinene, β pinene, isoprene) strongly dependent on the first axis ($0.98 < r^2 < 0.99$), suggesting the presence of a source linked to biogenic activities originating from vegetation. On the other hand, the second group, comprising O₃, VOCs and NO_x anthropogenic, indicates a source from combustion activities ($0.83 < r^2 < 0.89$), which favors O₃ photochemistry. At CP, LT and Sk sites, the pollutant category in which O₃ is found is linked to biogenic emissions (VOCs) and combustion sources. At these sites, temperature, humidity, precipitation and radiation are anti-correlated with O₃ ($-0.90 < r < -0.43$) (Table 5). High O₃ concentrations are therefore measured at these sites during the driest and coldest months (Swartz et al., 2020b). The main contributions are BVOCs, NO_x and anthropogenic VOCs, temperature and rainfall at CP, VOCs, humidity, temperature at Sk, NO_x and anthropogenic VOCs, and radiation at Af and anthropogenic VOCs, radiation, humidity at LT. These factors contribute between 5.1% and 39.4% (Fig. 14) to the formation of the axes, with a good representation quality (0.44 to 0.97) for most of them. Observations made at South African sites are confirmed by several recent studies. Indeed, Swartz et al. (2020b) attributed the decrease in O₃ concentrations from 1995 to 2001 to the decrease in NO₂ concentrations over this period at LT. The importance of humidity and temperature in O₃ photochemistry observed at almost all South African sites has been highlighted by Balachov et al. (2014), Laban et al. (2018, 2020). Laban et al. (2018) added that emissions from domestic combustion (in winter) and regional biomass combustion (in spring) are also responsible for the increase of O₃ levels. The contribution of VOCs to O₃ photochemistry in South Africa is confirmed by Jaars et al. (2016). At Mb, neither of the two



540 main axes has a significant relationship with O₃, with a poor quality of representation on the main axes (0.14). Further studies on other precursors such as biogenic NO and carbon monoxide (CO) should be carried out, and biomass combustion on a continental scale should also be taken into account, in order to better assess the dominant chemical contributions to O₃ production at this site.



545

Figure 14. Contribution of different variables to photochemical O₃ pollution in (a) Dry savanna (b) West savanna and Forest (c) Agricultural/semi-arid savanna.

550 **Table 5.** Correlation r between O₃, its precursors and meteorological variables at different sites. Blank spaces in the table indicate the absence of data on this site for the precursor concerned over the study period.

Ecosystem	Dry savanna					Wet savanna		Forest		Agricultural/semi-arid savanna				
Sites	Ba	Ka	Ag	Bb	Da	La	Dj	Zo	Bo	Mb	LT	CP	Af	Sk
	O ₃													
NO biogenic	0.85	0.73	0.92	-	-	-0.15	-0.24	0.43	-10 ⁻³	-	-	-	-	-
NOx_C	-0.33	-0.43	0.04	-	0.001	0.49	0.059	0.80	-0.33	0.31	0.37	-0.67	0.62	0.61
VOC_C	-0.40	-0.47	-0.003	-	-5.10 ⁻⁴	0.54	0.05	0.79	-0.40	0.31	0.60	-0.87	0.52	0.65
isoprene	0.51	0.54	0.46	0.79	0.78	0.92	0.81	0.80	0.92	0.42	-0.39	-0.91	0.29	-0.64
α pinene	0.67	0.76	0.66	0.45	0.77	0.74	0.64	0.63	0.90	0.36	-0.45	-0.86	0.29	-0.67
β pinene	0.70	0.79	0.72	0.34	0.72	0.70	0.56	0.60	0.89	0.33	-0.48	-0.85	0.27	-0.71
Temperature	0.45	0.47	0.42	0.51	0.76	0.72	0.69	0.68	0.89	0.47	-0.46	-0.90	0.49	-0.62
Humidity	0.82	0.64	0.95	0.52	0.70	-0.85	-0.19	-0.89	-0.79	-0.61	-0.79	-0.68	0.1	-0.80
Rainfall	0.74	0.64	0.75	0.15	0.51	-0.48	-0.39	-0.76	-0.54	-0.18	-0.49	0.74	0.53	-0.69
Radiation	0.16	0.15	0.26	0.75	0.69	0.73	0.54	0.65	0.87	0.21	-0.19	-0.76	0.71	-0.43

3.5 Annual and seasonal trends of O₃ and its precursors

3.5.1 Annual trends

555 Annual trends in O₃ concentrations were calculated according to Mann-Kendall test (Fig. 15). At the annual scale, Ka site in Mali shows a significant decrease in O₃ concentrations around -0.24 ppb yr⁻¹ (-2.3 % yr⁻¹) from 2001 to 2020 (pvalue = 0.002) at the 95% confidence level. At the seasonal scale, this downward trend at Ka is confirmed in both the dry and wet seasons. O₃ concentrations decrease by -0.18 ppb (-2.1 % yr⁻¹; pvalue = 0.03) per year in the dry season and -0.33 ppb (-2.4 % yr⁻¹; pvalue < 0.01) in the wet season. At the same site, the trend in nitrogen oxide (NO₂) over the 1998-2020 period shows a decline in annual concentrations and annual seasonal means. Ossouhou et al. (2019) observed a decrease in NO₂ concentrations at Ka

560



in the wet season of $-0.04 \text{ ppb yr}^{-1}$ ($-2.4 \% \text{ yr}^{-1}$) over the period 1998-2015. These downward trends in NO_2 could therefore explain the downward trends in O_3 . At the Ba site during the dry period, a significant downward trend is recorded, with O_3 decreasing by $-0.15 \text{ ppb yr}^{-1}$ ($-1.9 \% \text{ yr}^{-1}$; p value = 0.04). Calculation of trends on biogenic VOCs at Ba indicate a decrease in biogenic emissions of alpha pinene ($\tau = -0.37$, p value = 0.020) and beta pinene ($\tau = -0.39$, p value = 0.01). Chen et al. (2018) indicated that trends in global tree cover from 2000 to 2015 have led to clear decreases, particularly in West Africa with a reduction of around 10% in regional BVOC emissions due to agricultural expansion. At the other sites, no significant trends were observed. The absence of annual trends at South African sites confirms the results obtained by Swartz et al. (2020a, 2020b) at the LT, Af, Sk and CP sites. Breaks in the annual concentration data were observed at Ba and Ka in 2006 as a result of the Pettitt test. During the dry and wet seasons, further breaks were recorded in the annual series in 2006 (Ka) and 2007 (Ba) (dry season) and in 2014 at Ka (wet season). However, no trend inversion was induced in these break years. At the other study sites, no breaks were observed.

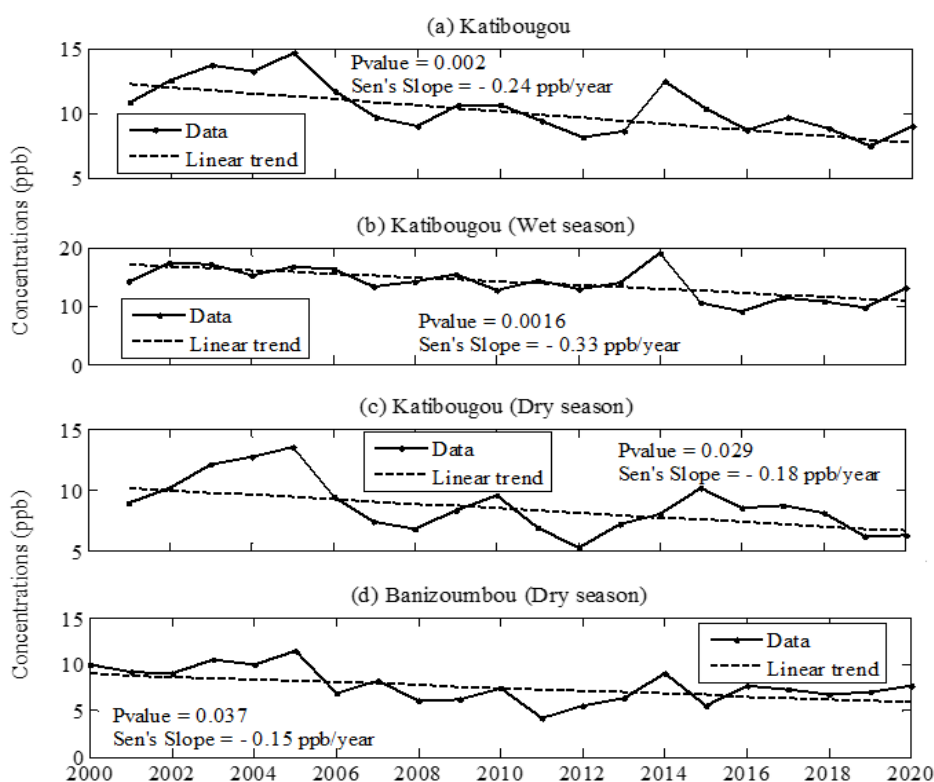


Figure 15. Significant long-term annual linear trend in in situ O_3 concentrations over the period 2000-2020

575

3.5.2 Seasonal trend

Trend tests are performed on monthly mean O_3 concentrations using seasonal Kendall test and significant trend results are presented in Fig. 16. The test reveals downward trends of $-0.07 \text{ ppb yr}^{-1}$ ($-0.6 \% \text{ yr}^{-1}$; p value = 0.02) at Ba and $-0.24 \text{ ppb yr}^{-1}$ ($-2.3 \% \text{ yr}^{-1}$; p value < 0.001) at Ka for a 95% confidence level. A significant upward trend is reported at Zo in Cameroon (Sen slope = 0.1 ppb yr^{-1} ; $1.4 \% \text{ yr}^{-1}$; p value = 0.001), and at Sk in South Africa (Sen slope = 0.3 ppb yr^{-1} ; $1.5 \% \text{ yr}^{-1}$; p value = 0.001). To explain the trends observed at Zo, we apply the Kendall rank correlation between O_3 concentrations and its precursors. We obtain a significant positive rank correlation at the 95% confidence level. For NO_x and anthropogenic VOCs,

580



585 $\tau = 0.7$ (pvalue= 0.03) while with biogenic VOCs, the correlation varies from 0.54 to 0.69 (pvalue <0.01). In addition, we observe increasing trends for biogenic VOCs. Isoprene increases by $1.8 \text{ ng.m}^{-2}\text{s}^{-1}$ per year (pvalue = 0.001), alpha pinene by $0.1 \text{ ng.m}^{-2}\text{s}^{-1}$ (pvalue < 0.001) and beta pinene by $0.04 \text{ ng.m}^{-2}\text{s}^{-1}$ (pvalue = 0.003). Similar trends were also observed in the wet season for alpha pinene and beta pinene, and in the dry season for isoprene. The significant rise in O_3 concentrations in Zo could therefore be explained by these increasing trends observed in isoprene, alpha pinene and beta pinene from one season to the next and in anthropogenic emissions in African forest regions. These results are corroborated by 18 years of satellite data (1998-2015) used by Andela et al. (2017) who noted an increasing trend in burned areas in dense canopy forests. At Sk, the upward trend is thought to be due to anthropogenic and biogenic emissions. At the Irene site in the North-eastern interior of South Africa, Bencherif et al. (2020) obtained an upward trend in the tropospheric O_3 column at a rate of around 2.4% per decade. In addition, an upward trend in NO_2 levels was also evident at Sk, signifying the influence of growing rural communities on the Kruger National Park border (Swartz et al., 2020b). This population growth and the associated increase in anthropogenic activities could therefore justify the upward trend obtained.

595

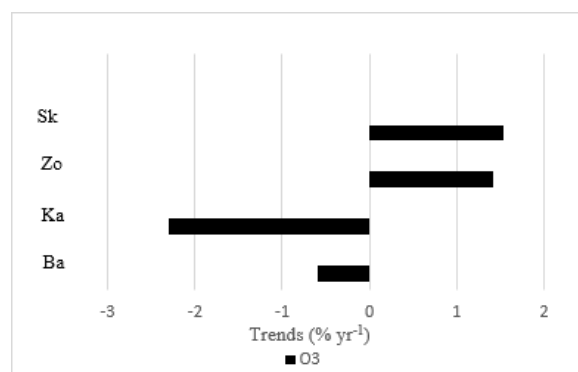


Figure 16 Significant Kendall's seasonal trend for O_3 Concentrations

4. Conclusion

600 This work presents an original database of long-term O_3 concentrations at fourteen African sites belonging to the INDAAF program and companion projects. This database gives a better understanding of O_3 concentration levels at remote tropical sites representative of the major African biomes. In this study, we establish a mean annual cycle by site and ecosystem type, and investigate the seasonal variability of O_3 concentrations over the period 1995-2020. Our analysis of the seasonality of anthropogenic and biogenic NO_x and VOC emissions then highlights the significant factors contributing to O_3 formation. Finally, we calculate the O_3 long-term trends, which provide an insight into the long-term evolution of O_3 levels and the local and regional dynamics of the emission sources of its precursors.

The results indicated that O_3 levels are the highest during the rainy season in dry savannas and during the dry season in wet savannas and forests. In agricultural fields, no seasonal variations of O_3 concentrations are observed. In semi-arid savanna (South Africa), dry season O_3 levels are the highest at LT and Sk. At CP and Af sites, maxima occur during the rainy season. Mean annual O_3 concentrations range from 10.5 ± 5.4 to 14.8 ± 4.3 ppb in dry savannas, from 10.8 ± 3.3 to 13.5 ± 4.8 ppb in wet savannas, from 3.9 ± 1.1 to 5.2 ± 2.1 ppb in forest ecosystems and from 19.9 ± 4.7 to 29.1 ± 8.4 ppb in semi-arid/agricultural savannas. BVOC (under the influence of air temperature), NO emissions (in the presence of humidity) and precipitation, are the main contributors to O_3 formation in dry savannas. The seasonality of O_3 measurements and dominant precursors confirm the important role of microbial processes leading to high NO emissions at the beginning of the wet season for O_3 production. Furthermore, the influence of air temperature and solar radiation on woody emissions from shrubs in the Sahel, and the presence of sparse vegetation (short grasses, forbs and dicotyledonous shrubs with perennial ground cover) in this region could

615



620 be at the origin of BVOC emissions. The photochemical O₃ regime in savannas and rainforests (heavily vegetated areas) is strongly linked to BVOC emissions from vegetation, and to temperature, radiation and humidity. At La and Zo, anthropogenic NO_x and VOC also contribute to O₃ formation. The most dominant precursor species in southern Africa are mainly VOC emissions (anthropogenic and biogenic), humidity and temperature, as well as anthropogenic NO_x at a few sites. They are due of Biomass and fuel combustion, large-scale transport of pollutants, domestic combustion in winter and biogenic emissions from vegetation. At INDAAF sites, which are rural sites far from many anthropogenic sources, O₃ concentrations are below most of the values reported in the literature. Annual and seasonal Mann-Kendall trends at all sites indicate that the Ka site in Mali and the Ba site in Niger experience a significant decrease in O₃ concentrations (around -2.3 % yr⁻¹ and -0.6% yr⁻¹) over
625 the period 2000 to 2020 justified by downward trends of NO₂ trends observed at Ka and the BVOC emissions at Ba. In contrast, a significant upward trend is reported at Zo (1.4% yr⁻¹) in Cameroon and Sk (1.5% yr⁻¹) in South Africa. These trends could be attributed to the increase in BVOCs in Zo and anthropogenic and biogenic emissions in Sk.

This study described in details the O₃ levels in representative African biomes, as well as the photochemical regimes and conditions leading to the observed concentrations. The results presented in this article constitute a robust database showing the
630 importance of developing or maintaining long-term observation projects and observatories. This database could be used to assess the impact of O₃ dry deposition fluxes on African crops and the potential yield losses because of O₃ absorption by crops. An assessment of the various agricultural losses during the growing season will help to better orient actions to improve crop yield and achieve food security. In addition, this documentation is invaluable for modeling chemical processes in the atmosphere and for projecting future changes in tropospheric O₃. It could limit the uncertainties of these models and facilitate
635 their validation, which is mainly based on data measured in situ.

Data availability. The INDAAF O₃ observations are available on the program website at <https://indaaf.obs-mip.fr> (<https://doi.org/10.25326/608> ; <https://doi.org/10.25326/604> ; <https://doi.org/10.25326/610> ; <https://doi.org/10.25326/609> ; <https://doi.org/10.25326/606> ; <https://doi.org/10.25326/275> ; <https://doi.org/10.25326/605> ; <https://doi.org/10.25326/603> ;
640 <https://doi.org/10.25326/607> ; <https://doi.org/10.25326/642> ; <https://doi.org/10.25326/646> ; <https://doi.org/10.25326/645> ; <https://doi.org/10.25326/644> ; <https://doi.org/10.25326/647>). GFED4 (NO_x, COV) and MEGAN-MACC (Isoprene, pinene-a, pinene-b) data are available from <https://eccad.sedoo.fr/#/data>. ERA5 reanalysis data are available from <https://cds.climate.copernicus.eu/cdsapp#!/dataset/reanalysis-era5-single-levels?tab=overview>.

645 **Author contributions.** CGL designed the study, wrote the protocol and edited the paper. HEVD conducted data processing, the statistical analysis and wrote the paper. CD made conceptual contributions and edited the paper. ABA and MO contributed at the statistical analysis, assisted in sample collection and edited the paper. VY, DL, MO-L, ON, PGVZ assisted in sample collection and edited the paper. EG and MDA analysed the samples.

650 **Competing interests.** The contact author has declared that none of the authors has any competing interests.

Disclaimer.

655 **Acknowledgements.** The authors would like to acknowledge the INDAAF project (International Network to study Deposition and Atmospheric chemistry in Africa), and especially all its local technicians for their maintenance and sampling work. We would also like to acknowledge the "Cycle de l'Azote entre la Surface et l'Atmosphère en Afrique" (CASAQUE) project and the Integrated Nitrogen Management system (INMS) for providing us with data on O₃ concentrations at Dahra and Mbita. This study was supported by the INSA (Integrated Nitrogen Studies in Africa) project, which funded the research carried out for this paper at the "Laboratoire d'Aérodynamique de Toulouse". We are indebted to the AMMA-CATCH project, the University of
660 Copenhagen and the Observatoire de recherche en environnement "Bassins versants tropicaux expérimentaux" (SO BVET)



for providing us with meteorological data from Niger, Benin, Senegal and Cameroon. We are also grateful to the ECCAD platform and the European Centre for Medium-Range Weather Forecasts (ECMWF) for biogenic and anthropogenic emissions and ERA5 reanalysis data.

665 **Financial support.** This study has received funding from the European Union's Horizon 2020 research and innovation programme under the Marie Skłodowska-Curie grant agreement no. 871944.

Review statement.

670 References

- Abbadie, L. (Ed.), Lamto: Structure, Functioning, and Dynamics of a Savanna Ecosystem, Ecological Studies, Springer Science+Business Media, New York, 415pp., ISBN: 9780387948447, 2006.
- Abiodun, B. J., Ojumu, A. M., Jenner, S., Ojumu, T. V.: The transport of atmospheric NO_x and HNO₃ over Cape Town, Atmos. Chem. Phys., 14, 559–575, <https://doi.org/10.5194/acp-14-559-2014>, 2014.
- 675 Adon, M., Galy-Lacaux, C., Delon, C., Yoboue, V., Solmon, F., and Kaptue T. A, T.: Dry deposition of nitrogen compounds (NO₂, NO₃, NH₃), sulfur dioxide and ozone in west and central African ecosystems using the inferential method, Atmos. Chem. Phys., 13, 11351–11374, 2013.
- Adon, M., Galy-Lacaux, C., Yoboué, V., Delon, C., Lacaux, J. P., Castera, P., Gardrat, E., Pienaar, J., Al Ourabi, H., Laouali, D., Diop, B., Sigha-Nkamdjou, L., Akpo, A., Tathy, J. P., Lavenu, F., and Mougín, E.: Long term measurements of sulfur dioxide, nitrogen dioxide, ammonia, nitric acid and ozone in Africa using passive samplers, Atmos. Chem. Phys., 10, 7467–7487, doi:10.5194/acp-10-7467-2010, 2010.
- 680 Adon, M., Yoboue, V., Galy-Lacaux, C., Liousse, C., Diop, B., Doumbia, E. H. T., Gardrat, E., Ndiaye, S. A., and Jarnot, C.: Measurements of NO₂, SO₂, NH₃, HNO₃ and O₃ in West African urban environments, Atmos. Environ., 135, 31–40, <https://doi.org/10.1016/j.atmosenv.2016.03.050>, 2016.
- 685 Aghedo, A. M., Schultz, M. G., and Rast, S.: The influence of African air pollution on regional and global tropospheric ozone, Atmos. Chem. Phys., 7, 1193–1212, <https://doi.org/10.5194/acp-7-1193-2007>, 2007.
- Aït-Sahalia, Y. and Xiu, D.: Principal Component Analysis of High-Frequency Data. Journal of the American Statistical Association, 114, 287–303, <https://doi.org/10.1080/01621459.2017.1401542>, 2019.
- Akpo, A. B., Galy-Lacaux, C., Laouali, D., Delon, C., Liousse, C., Adon, M., Gardrat, E., Mariscal, A., Darakpa, C.: Precipitation chemistry and wet deposition in a remote wet savanna site in West Africa: Djougou (Benin), Atmospheric Environment, 115, 110–123, 2015, <http://dx.doi.org/10.1016/j.atmosenv.2015.04.064>
- 690 Alves, E. G., Jardine, K., Tota, J., Jardine, A., Yáñez-Serrano, A. M., Karl, T., et al. : Seasonality of isoprenoid emissions from a primary rainforest in central Amazonia, Atmospheric Chemistry and Physics, 16, 3903–3925. <https://doi.org/10.5194/acp-16-3903>, 2016
- Andela, N., Morton, C., Giglio, L., Chen, Y., van Der Werf, G., Kasibhatla, P. S., DeFries, R. S., Collatz, G. J., Hantson, S., Kloster, S., 695 Bachelet, D., Forrest, M., Lasslop, G., Li, F., Mangeon, S., Melton, J. R., Yue, C., Randerson, J. T.: A human-driven decline in global burned area, Science, 356, 1356–1362, <https://doi.org/10.1126/science.aal4108>, 2017.
- Bahino, J., Yoboué, V., Galy-Lacaux, C., Adon, M., Akpo, M., Liousse, C., Gardrat, E., Chiron, C., Ossohou, M., Gnamien, S., Keita, S., and Djossou, J.: A pilot study of gaseous pollutants' measurement (NO₂, HNO₃, SO₂, NH₃ and O₃) in Abidjan, Côte d'Ivoire: contribution to an overview of gaseous pollution in African cities, Atmos. Chem. Phys., 18, 5173–5198, <https://doi.org/10.5194/acp-18-5173-2018>, 700 2018.
- Baglama, J., Reiche, L. and Lewis, B. W.: Fast Truncated Singular Value Decomposition and Principal Components Analysis for Large Dense and Sparse Matrices. R package version 2.3.5, URL: <https://CRAN.Rproject.org/package=irlba>, 2021.
- Balashov, N. V., Thompson, A. M., Piketh, S. J., and Langerman, K. E.: Surface ozone variability and trends over the South African Highveld from 1990 to 2007, J. Geophys. Res.-Atmos., 119, 4323–4342, <https://doi.org/10.1002/2013JD020555>, 2014.
- 705 Baldy, S., Ancellet, G., Bessafi, M., Badr, A., and Luk, D. L. S.: Field observations of the vertical distribution of tropospheric ozone at the island of Reunion (southern tropics), J. Geophys. Res.-Atmos., 101, 23835–23849, doi:10.1029/95jd02929, 1996.
- Bakayoko, A., Galy-Lacaux, C., Véronique Yoboué, V., Hickman, J. E., Roux, F., Gardrat, E., Julien, F., and Delon, C.: Dominant contribution of nitrogen compounds in precipitation chemistry in the Lake Victoria catchment (East Africa), Environ. Res. Lett, 16, 1–20, doi 10.1088/1748-9326/abe25c, 2021.
- 710 Bencherif, H., Tohir, A. M., Mbatha, N., Sivakumar V., Preez, D. J., Bègue, N., and Coetzee, G.: Ozone Variability and Trend Estimates from 20-Years of Ground-Based and Satellite Observations at Irene Station, South Africa, Atmosphere, 11, 1216, doi:10.3390/atmos11111216, 2020.



- Bigaignon, L., Delon, C., Ndiaye, O. Galy-Lacaux, C., Serça, D., Guérin, F., Talleg, T., Merbold, L., Tagesson, T., Fensholt, R., André, S. and Sylvain Galliau, S.: Understanding N₂O Emissions in African Ecosystems: Assessments from a Semi-Arid Savanna Grassland in Senegal and Sub-Tropical Agricultural Fields in Kenya, *Sustainability*, MDPI, 12, 1–26, doi:10.3390/su12218875, 2020.
- Boiyo, R., Kumar, K. R., Zhao, T. and Bao, Y. : Climatological analysis of aerosol optical properties over East Africa observed from spaceborne sensors during 2001–2015, *Atmos. Environ.*, 152, 298–313, <https://doi.org/10.1016/j.atmosenv.2016.12.050>, 2017b.
- Bruno, P., Caselli, M., de Gennaro, G. and Traini, A.: Source apportionment of gaseous atmospheric pollutants by means of an absolute principal component scores (APCS) receptor model, *Fresenius J. Anal. Chem.*, 371, 1119–1123, doi:10.1007/s002160101084, 2001.
- Carmichael, G. R., Streets, D. G., Calori, G., Amann, M., Jacobson, M. Z., Hansen, J., and Ueda, H.: Changing trends in sulfur emissions in Asia: Implications for acid deposition, *Environ. Sci. Technol.*, 36, 4707–4713, doi:10.1021/es011509c, 2002.
- Camredon, M. and Aumont, B.: I-L'ozone troposphérique : production/consommation et régimes chimiques, *Pollut. Atmos.*, 193, 51–60 doi:10.4267/pollution-atmosphérique.1404, 2007.
- Carmichael, G.R., Ferm, M., Thongboonchoo, N., Woo, J.-H., Chan, L., Murano, K., Viet, P.H., Mossberg, C., Bala, R., Boonjawat, J., Upatum, P., Mohan, M., Adhikary, S.P., Shrestha, A.B., Pienaar, J., Brunke, E.B., Chen, T., Jie, T., Guoan, D., Peng, L.C., Dhiharto, S., Harjanto, H., Jose, A.M., Kimani, W., Kirouane, A., Lacaux, J.-P., Richard, S., Barturen, O., Cerda, J.C., Athayde, A., Tavares, T., Cotrina, J.S., Bilici, E. : Measurements of sulfur dioxide, ozone and ammonia concentrations in Asia, Africa, and South America using passive samplers, *Atmos. Environ.*, 37, 1293–1308. [https://doi.org/10.1016/S1352-2310\(02\)01009-9](https://doi.org/10.1016/S1352-2310(02)01009-9), 2003.
- Chang, K.-L., Petropavlovskikh, I., Cooper, I. O. R., Schultz, M. G., and Wang, T.: Regional trend analysis of surface ozone observations from monitoring networks in eastern North America, Europe and East Asia, *Elem Sci Anth*, 50, 1–22, doi: <https://doi.org/10.1525/elementa.243>, 2017.
- Chen, W. H., Guenther, A. B., Wang, X. M., Chen, Y. H., Gu, D. S., Chang, M., Zhou, S. Z., Wu, L. L., Zhang, Y. Q.: Regional to global biogenic isoprene emission responses to changes in vegetation from 2000 to 2015, *Journal of Geophysical Research: Atmospheres*, 123, 3757–3771, <https://doi.org/10.1002/2017JD027934>, 2018.
- Clain, G., Baray, J. L., Delmas, R., Diab, R., Leclair de Bellevue, J., Keckhut, P., Posny, F., Metzger, J. M., and Cammas J. P.: Tropospheric ozone climatology at two Southern Hemisphere tropical/subtropical sites, (Reunion Island and Irene, South Africa) from ozone sondes, LIDAR, and in situ aircraft measurements, *Atmos. Chem. Phys.*, 9, 1723–1734, <https://doi.org/10.5194/acp-9-1723-2009>, 2009.
- Cooper, O. R., Schultz, M. G., Schröder, S., Chang, K.-L., Gaudel, A., Benítez, G. C., Cuevas, E., Fröhlich, M., Galbally, I. E., Molloy, S., Kubistin, D. Lu, X., McClure-Begley, A., Nédélec, P., O'Brien, J., Oltmans, S. J., Petropavlovskikh, I., Ries, L., Senik, I. Sjöberg, K., Solberg, S., Spain, G. T., Spang, W., Steinbacher, M., Tarasick, D., Thouret V., and Xu, X.: Multi-decadal surface ozone trends at globally distributed remote locations, *Elem Sci Anth*, 8, 1–34, DOI: <https://doi.org/10.1525/elementa.420>, 2020
- Cooper, O. R., Parrish, D. D., Ziemke, J., Balashov, N. V., Cupeiro, M., Galbally, I. E., Gilge, S., Horowitz, L., Jensen, N. R., Lamarque, J.-F., Naik, V., Oltmans, S. J., Schwab, J., Shindell, D. T., Thompson, A. M., Thouret, V., Wang, Y., Zbinden, R. M.: Global distribution and trends of tropospheric ozone: An observation-based review, *Elementa*, 2, 1–28, DOI: <https://doi.org/10.12952/journal.elementa.000029>, 2014.
- Conradie, E. H., Van Zyl, P. G., Pienaar, J. J., Beukes, J. P., Galy-Lacaux, C., Venter, A. D., and Mkhathshwa, G. V.: The chemical composition and fluxes of atmospheric wet deposition at four sites in South Africa, *Atmos. Environ.*, 146, 113–131, <https://doi.org/10.1016/j.atmosenv.2016.07.033>, 2016.
- Cros, B., Fontan, J., Minga, A., Helas, G., Nganga, D., Delmas, R., Chapuis, A., Benech, B., Druilhet, A., and Andreae, M. O.: Vertical profiles of ozones between 0 and 400 meters in and above the African equatorial Forest, *J. Geophys. Res.*, 97, 12877–12887, 1992.
- Darras, S., Granier, C., Lioussé, C., Doumbia, T., Keita, S., Soulie, A.: The ECCAD database: Access to a variety of inventories of emissions for greenhouse gases and air pollutants, 35ème colloque annuel de l'Association Internationale de Climatologie – AIC, France, 6–9 July 2022, 1–6, 2022.
- Debaje, S. B., Jeyakumar, S. J., Ganesan, K., Jadhav, D. B., and Seetaramayya, P.: Surface ozone measurements at tropical rural coastal station Tranquebar, India, *Atmos. Environ.*, 37, 4911–4916, <https://doi.org/10.1016/j.atmosenv.2003.08.005>, 2003.
- Delon, C., Galy-Lacaux, C., Adon, M., Lioussé, C., Serça, D., Diop, B., and Akpo, A.: Nitrogen compounds emission and deposition in West African ecosystems: comparison between wet and dry savanna *Biogeosciences*, 9, 385–402, 2012. doi:10.5194/bg-9-385-2012, 2012.
- Delon, C., Galy-Lacaux, C., Barret, B., Ndiaye, O., Serça, D., Guérin, F., Gardrat, E., Mougín, E., Agbohessou, Y. F., Probst, A.: Nitrogen budget and critical load determination at a Sahelian grazed grassland site, *Nutr Cycl Agroecosyst*, 124, 17–34, <https://doi.org/10.1007/s10705-022-10220-6>, 2022.
- Delon, C., Galy-Lacaux, C., Boone, A., Lioussé, C., Serça, D., Adon, M., Diop, B., Akpo, A., Lavenu, F., Mougín, E., and Timouk, F.: Atmospheric nitrogen budget in Sahelian dry savannas, *Atmos. Chem. Phys.*, 10, 2691–2708, <https://doi.org/10.5194/acp-10-2691-2010>, 2010.
- Delon, C., Mougín, E., Serça, D., Grippa, M., Hiernaux, P., Diawara, M., Galy-Lacaux, C., Kergoat, L.: Modelling the effect of soil moisture and organic matter degradation on biogenic NO emissions from soils in Sahel rangeland (Mali), *Biogeosciences*, 12, 3253–3272. <https://doi.org/10.5194/bg-12-3253-2015>, 2015.



- Dufour, G., Hauglustaine, D., Zhang, Y., Eremanko, M., Cohen, Y., Siour, G., Lachatre, M., Bense, A., Bessagnet, B., Cuesta, J., Thouret, V., and Zheng, B., Gaudel, A., Ziemke, J.: Recent ozone trends in the Chinese free troposphere: role of the local emission reductions and meteorology. *Atmos. Chem. Phys.*, 21, 16001–16025, <https://doi.org/10.5194/acp-21-16001-2021>, 2021.
- 770 Duriš, V., Bartková, R., Tirpáková, A.: Principal Component Analysis and Factor Analysis for an Atanassov IF Data Set. *Mathematics*, 9, 1–12. <https://doi.org/10.3390/math9172067>, 2021.
- Ferm, M.: A Sensitive Diffusional Sampler, IVL Report L91, Göteborg, Swedish Environmental Research Institute, Sweden, 12pp, ISSN 0283-877X, 1991.
- Ferm, M., Rodhe, H.: Measurements of Air Concentrations of SO₂, NO₂ and NH₃ at Rural and Remote Sites in Asia, *Journal of atmospheric chemistry*, 27, 17–29, <http://dx.doi.org/10.1023/A:1005816621522>, 1997.
- 775 Ferreira, J., Reeves, C. E., Murphy, J. G., Garcia-Carreras, L., Parker, D. J., and Oram, D. E.: Isoprene emissions modelling for West Africa: MEGAN model evaluation and sensitivity analysis, *Atmos. Chem. Phys.*, 10, 8453–8467, <https://doi.org/10.5194/acp-10-8453-2010>, 2010
- Fleming, Z. L., Doherty, R. M., von Schneidmesser, E., Malley, C. S., Cooper, O. R., Pinto, J. P., Colette, A., Xu, X., Simpson, D., Schultz, M. G., Lefohn, A. S., Hamad, S., Moolla, R., Solberg, S., and Feng, Z.: Tropospheric Ozone Assessment Report: Present-day ozone distribution and trends relevant to human health, *Elem Sci Anth*, 6, 1–41 DOI: <https://doi.org/10.1525/elementa.273>, 2018.
- 780 Fowler, D., Pilegaard, K., Sutton, M.A., Ambus, P., Raivonen, M., Duyzer, J., Simpson, D., Fagerli, H., Fuzzi, S., Schjoerring, J.K., Granier, C., Neftel, A., Isaksen, I.S.A., Laj, P., Maione, M., Monks, P.S., Burkhardt, J., Daemmgen, U., Neiryneck, J., Personne, E., Wichink-Kruit, R., Butterbach-Bahl, K., Flechard, C., Tuovinen, J.P., Coyle, M., Gerosa, G., Loubet, B., Altimir, N., Gruenhage, L., Ammann, C., Cieslik, S., Paoletti, E., Mikkelsen, T.N., Ro-Poulsen, H., Cellier, P., Cape, J.N., Horvath, L., Loreto, F., Niinemets, Ü., Palmer, P.I., Rinne, J., Misztal, P., Nemitz, E., Nilsson, D., Pryor, S., Gallagher, M.W., Vesala, T., Skiba, U., Brüggemann, N., Zechmeister-Boltenstern, S., Williams, J., O’ Dowd, C., Facchini, M.C., De Leeuw, G., Flossman, A., Chaumerliac, N., Erisman, J.W. : Atmospheric composition change: ecosystems-Atmosphere interactions, *Atmos. Environ.* 43, 5193–5267. <https://doi.org/10.1016/j.atmosenv.2009.07.068>, 2009.
- 785 Frimpong, B. F., Koranteng, A., and Molkenthin, F.: Analysis of temperature variability utilising Mann–Kendall and Sen’s slope estimator tests in the Accra and Kumasi Metropolises in Ghana. *Environmental Systems Research*, 11, 1–13, <https://doi.org/10.1186/s40068-022-00269-1>, 2022.
- Galanter, M., Levy I. I., H., and Carmichael, G. R.: Impacts of biomass burning on tropospheric CO, NO_x, and O₃, *J. Geophys. Res.*, 105, 6633–6653, doi: 10.1029/1999JD901113, 2000.
- 795 Galy-Lacaux, C., Laouali, D., Descroix, L., Gobron, N., Lioussé, C.: Long term precipitation chemistry and wet deposition in a remote dry savanna site in Africa (Niger). *Atmos. Chem. Phys.*, 9, 1579–1595, <https://doi.org/10.5194/acp-9-1579-2009>, 2009.
- Galy-Lacaux, C. and Modi, A.I.: Precipitation Chemistry in the Sahelian Savanna of Niger, Africa, *Journal of Atmospheric Chemistry*, 30, 319–343, 1998.
- García-Lázaro, J., Moreno-Ruiz, J., Riaño, D., Arbelo, M.: Estimation of burned area in the northeastern siberian boreal forest from a long-term data record (LTDR) 1982–2015 time series. *Rem. Sens.* 10, 1–15, <https://doi.org/10.3390/rs10060940>, 2018.
- 800 Gaudel, A., Cooper, O. R., Ancellet, G., Barret, B., Boynard, A., Burrows, J. P., Clerbaux, C., Coheur, P.-F., Cuesta, Cuevas, J. E., Doniki, S., Dufour, Ebojje, G. F., Foret, Garcia, G. O., Granados-Muñoz, M. J., Hannigan, J. W., Hase, F., Hassler, B., Huang, G., Hurtmans, D., Jaffe, D., Jones, N., Kalabokas, P., Kerridge, B., Kulawik, S., Latter, B., Leblanc, T., Le Flochmoën, E., Lin, W., Liu, J., Liu, X., Mahieu, E., McClure-Begley, A., Neu, J. L., Osman, M., Palm, M., Petetin, H., Petropavlovskikh, I., Querel, R., Rapp, R. N., Rozanov, A., Schultz, M. G., Schwab, J., Siddans, R., Smale, D., Steinbacher, M., Tanimoto, H., Tarasick, D. W., Thouret, V., Thompson, A. M., Trick, T., Weatherhead, E., Wespes, C., Worden, H. M., Vigouroux, C., Xu, X., Zeng, G., Ziemke, J.: Tropospheric Ozone Assessment Report: Present-day ozone distribution and trends relevant to climate and model evaluation, *Elem Sci Anth*, 6, 1–58, DOI: <https://doi.org/10.1525/elementa.291>, 2018.
- 805 Gaudel, A., Cooper, O. R., Chang, K.-L., Bourgeois, I., Ziemke, J. R., Strode, S. A., Oman, L. D., Sellitto, P., Nédélec, P., Blot, R., Thouret, V., Granier, C.: Aircraft observations since the 1990s reveal increases of tropospheric ozone at multiple locations across the Northern Hemisphere, *Sci. Adv.*, 6, 1–11, DOI: 10.1126/sciadv.aba8272, 2020.
- Graedel, T. E., and P. J.: Crutzen.: *Atmospheric Change: An Earth System Perspective*, NY: W. H. Freeman and Company, New York, 446 pp, ISBN 0716723344, 1993.
- 810 Gray, C. M., Helmig, D., Fierer, N.: Bacteria and fungi associated with isoprene consumption in soil. *Elementa: Science of the Anthropocene*, 3, 1–10, doi: 10.12953/journal.elementa.000053, 2015.
- Guenther, A., Hewitt, C.N., Erickson, D., Fall, R., Geron, C., Graedel, T., Harley, P., Klinger, L., Lerdau, M., McKay, W.A., Pierce, T., Scholes, B., Steinbrecher, R., Tallamraju, R., Taylor, J., Zimmerman, P.A.: Global model of natural volatile organic compound emissions, *J. Geophys. Res.* 100, 8873–8892. <https://doi.org/10.1029/94JD02950>, 1995.
- 815 Guenther, A., Karl, T., Harley, P., Wiedinmyer, C., Palmer, P. I., and Geron, C.: Estimates of global terrestrial isoprene emissions using MEGAN (Model of Emissions of Gases and Aerosols from Nature), *Atmos. Chem. Phys.*, 6, 3181–3210, doi:10.5194/acp-6-3181, 2006



- Guenther, A. B., Zimmerman, P. R., Harley, P. C., Monson, R. K., & Fall, R.: Isoprene and monoterpene emission rate variability: Model evaluations and sensitivity analyses, *Journal of Geophysical Research*, 98, 12609–12617. <https://doi.org/10.1029/93jd00527>, 1993
- Hagenbjörk, A., Malmqvist, E., Mattisson, K., Sommar, N. J., Modig, L.: The spatial variation of O₃, NO, NO₂ and NO_x and the relation between them in two Swedish cities, *Environ. Monit. Assess.* 189, 161–172, <https://doi.org/10.1007/s10661-017-5872-z>, 2017.
- 825 Hamdun, A. M., and Arakaki T.: Analysis of Ground Level Ozone and Nitrogen Oxides in the City of Dar es Salaam and the Rural Area of Bagamoyo, Tanzania, *Open Journal of Air Pollution*, 4, 224–238, 2015.
- Heue, K.-P., Coldewey-Egbers, M., Delcloo, A., Lerot, C., Loyola, D., Valks, P., and van Roozendaal, M., : Trends of tropical tropospheric ozone from 20 years of European satellite measurements and perspectives for the Sentinel-5 Precursor, *Atmos. Meas. Tech.*, 9, 5037–5051, 2016.
- 830 Hirsch, R. M., Slack, J. R., Smith, R. A.: Techniques of trend analysis for monthly water quality data, *Water Resour. Res.* 18, 107–121. <https://doi.org/10.1029/WR018i001p00107>, 1982.
- Homyak P. M., Sickman, J. O., Miller, A. E., Melack, J. M., and Schimel, J. P., : Assessing N saturation in a seasonally dry chaparral watershed: Limitations of traditional indicators of N saturation, *Ecosystems*, 17: 1286–1305, 2014.
- Ihedike, C., Mooney, J. D., Fulton, J., and Ling, J.: Evaluation of real-time monitored ozone concentration from Abuja, Nigeria, *BMC Public Health*, 23, 1–7, <https://doi.org/10.1186/s12889-023-15327-1>, 2023.
- 835 Jaars, K., van Zyl, P. G., Beukes, J. P., Hellén, H., Vakkari, V., Josipovic, M., Venter, A. D., Räsänen, M., Knoetze, L., Cilliers, D. P., Siebert, S. J., Kulmala, M., Rinne, J., Guenther, A., Laakso, L., and Hakola, H.: Measurements of biogenic volatile organic compounds at a grazed savannah grassland agricultural landscape in South Africa, *Atmos. Chem. Phys.*, 16, 15665–15688, 2016.
- Jaegle, L., Martin, R. V., Chance, K., Steinberger, L., Kurosu, T. P., Jacob, D. J., Modi, A. I., Yoboue, V., Sigha-Nkamdjou, L., and Galy-Lacaux, C.: Satellite mapping of rain-induced nitric oxide emissions from soils, *J. Geophys. Res.*, 109, 1–10, doi:10.1029/2004JD004787, 2004.
- Jolliffe, I. T.: Principal component analysis. Springer New York, État de New York, 488p, <https://doi.org/10.1007/b98835>, 1986.
- Josipovic, M., Annegarn, H. J., Kneen, M. A., Pienaar, J. J. and Piketh, S. J.,: Concentrations, distributions and critical level exceedance assessment of SO₂, NO₂ and O₃ in South Africa, *Environmental Monitoring and Assessment*, 171, 181–196, DOI: 10.1007/s10661-009-1270-5, 2010.
- 845 Kai, R. F., Scholes, M. C., Piketh, S. J., Scholes, R. J.: Analysis of the first surface nitrogen dioxide concentration observations over the South African Highveld derived from the Pandora-2s instrument, *Clean air journal*, 32, 1–11, <http://dx.doi.org/10.17159/caj/2022/32/1.13242>, 2022.
- Kendall, M.G.: Rank Correlation Methods, fourth ed. Charles Griffin, 4th Edition, Charles Griffin, London, 1975.
- 850 Keita, S., Liousse, C., Assamoi, E.-M., Doumbia, T., N’Datchoh, E. T., Gnamié, S., Elguindi, N., Granier, C. and Yoboué, V., : African anthropogenic emissions inventory for gases and particles from 1990 to 2015, *Earth Syst. Sci. Data*, 13, 3691–3705, <https://doi.org/10.5194/essd-13-3691-2021>, 2021.
- Khoder, M. I., Diurnal, Seasonal and Weekdays-Weekends Variations of Ground Level Ozone Concentrations in an Urban Area in Greater Cairo. *Environmental Monitoring and Assessment*, 149, 349–362, <https://doi.org/10.1007/s10661-008-0208-7>, 2009.
- 855 Kimayu, J. M., Gikuma-Njuru, P., and Musembi, D. K., : Temporal and Spatial Variability of Tropospheric Ozone in Nairobi City, Kenya, *Physical Science International Journal*, 13, 1–12, DOI: 10.9734/PSIJ/2017/31452, 2017.
- Kiros F., Shakya K. M., Rupakheti M., Regmi R. P., Maharjan R., Byanju R. M., Naja M., Mahata K., Kathayat B., Peltier E. R., : Variability of Anthropogenic Gases: Nitrogen Oxides, Sulfur Dioxide, Ozone and Ammonia in Kathmandu Valley, Nepal, *Aerosol and Air Quality Research*, 16: 3088–3101, <https://doi.org/10.7275/9997447>, 2016.
- 860 Laakso, L., Vakkari, V., Virkkula, A., Laakso, H., Backman, J., Kulmala, M., Beukes, J. P., van Zyl, P. G., Tiitta, P., Josipovic, M., Pienaar, J. J., Chiloane, K., Gilardoni, S., Vignati, E., Wiedensohler, A., Tuch, T., Birmili, W., Piketh, S., Collett, K., Fourie, G. D., Komppula, M., Lihavainen, H., de Leeuw, G., and Kerminen, V.-M.: South African EUCAARI measurements: seasonal variation of trace gases and aerosol optical properties, *Atmos. Chem. Phys.*, 12, 1847–1864, <https://doi.org/10.5194/acp12-1847-2012>, 2012.
- 865 Laakso, L., Laakso, H., Aalto, P. P., Keronen, P., Petäjä, T., Nieminen, T., Pohja, T., Siivola, E., Kulmala, M., Kgabi, N., Molefe, M., Mabaso, D., Phalatse, D., Pienaar, K., and Kerminen, V.-M.: Basic characteristics of atmospheric particles, trace gases and meteorology in a relatively clean Southern African Savannah environment, *Atmos. Chem. Phys.*, 8, 4823–4839, <https://doi.org/10.5194/acp-8-4823-2008>, 2008.
- Laban, T. L., Van Zyl, P. G., Beukes, J. P., Mikkonen, S., Santana, L., Josipovic, M., Vakkari, Thompson, A. M., Kulmala, M. and Laakso L.: Statistical analysis of factors driving surface ozone variability over continental South Africa, *Journal of Integrative Environmental Sciences*, pp; 1–28, DOI:10.1080/1943815X.2020.1768550, 2020.
- 870 Laban, T. L., Van Zyl, P. G., Beukes, J. P., Vakkari, V., Jaars, K., Borduas-Dedekind, N., Josipovic, M., Thompson, A. M., Kulmala, M., Laakso, L., : Seasonal influences on surface ozone variability in continental South Africa and implications for air quality, *Atmos. Chem. Phys.*, 15491–15514. <https://doi.org/10.5194/acp-18-15491-2018>, 2018.
- Lacaux, J. P., Tathy, J. P., and Sigha, L.: Acid wet deposition in the tropics: two case studies using DEBITS measurements, *IGACTivities Newsletter of the International Global Atmospheric Chemistry Project, DEBITS Special 2*, 13–18, 2003.
- 875



- Lanz, V. A., Alfarrar, M. R., Baltensperger, U., Buchmann, B., Hueglin, C. and Prévôt, A. S. H.: Source apportionment of submicron organic aerosols at an urban site by factor analytical modelling of aerosol mass spectra, *Atmospheric Chem. Phys.*, 7, 1503–1522, doi: 10.5194/acp-7-1503-2007, 2007.
- Laville, P., Henault, C., Gabrielle, B., and Serca, D.: Measurement and modelling of NO fluxes over maize and wheat crops during their growing seasons: effect of crop management, *Nutr. Cycl. Agroecosyst.* 72, 159–171, doi: 10.1007/s10705-005-0510-5, 2005.
- 880 Lee, J. D., Squires, F. A., Sherwen, T., Wilde, S. E., Cliff, S. J., Carpenter, L. J., Hopkins, J. R., Bauguutte, S. J., Reed, C., Barker, P., Allen, G., Bannan, T. J., Matthews, E., Mehra, A., Percival, C., Heard, D. E., Whalley, L. K., Ronnie, G. V., Seldon, S., Ingham, T., Keller, C. A., Knowland, K. E., Nisbetj, E. G., and Andrewsab. S.: Ozone production and precursor emission from wildfires in Africa, *Environ. Sci.: Atmos.*, 1, 524–542., doi: 10.1039/D1EA00041A, 2021.
- 885 Lefohn, A. S., Malley, C. S., Smith, L., Wells, B., and Hazucha, M., : Tropospheric Ozone Assessment Report: Global ozone metrics for climate change, human health, and crop/ecosystem research, *Elem Sci Anth*, 6, 1–39 DOI: <https://doi.org/10.1525/elementa.279>, 2018.
- Lelieveld, J., Evans, J. S., Fnais, M., Giannadaki, D., and Pozzer, A.: The contribution of outdoor air pollution sources to premature mortality on a global scale, *Nature*, 525, 367–371, <https://doi.org/10.1038/nature15371>, 2015.
- Lin, M., Horowitz, L. W., Cooper, O. R., Tarasick, D., Conley, S., Iraci, L. T., Johnson, B., Leblanc, T., Petropavlovskikh, I., and Yates, E. L.: Revisiting the evidence of increasing springtime ozone mixing ratios in the free troposphere over western North America., *Geophys Res Lett* 42, 8719–8728. DOI: <https://doi.org/10.1002/2015GL065311>, 2015.
- Liu, Y., Schallhart, S., Taipale, D., Tykkä, T., Räsänen, M., Merbold, L., Hellén, H., and Pellikka, P.: Seasonal and diurnal variations in biogenic volatile organic compounds in highland and lowland ecosystems in southern Kenya, *Atmospheric Chemistry and Physics*, 21, 14761–14787, <https://doi.org/10.5194/acp-21-14761-2021>, 2021.
- 895 Lourens, A. S., Beukes, J. P., Van Zyl, P. G., Fourie, G. D., Burger, J. W., Pienaar, J. J., Read, C. E., and Jordaan, J. H.: Spatial and temporal assessment of gaseous pollutants in the Highveld of South Africa, *S. Afr. J. Sci.*, 107, 1–8, doi: 10.4102/sajs.v107i1/2.269, 2011.
- Lu, X., Zhang, L., Zhao, Y., Jacob, D. J., Hu, Y., Hu, L., Gao, M., Liu, X., Petropavlovskikh, I., McClure-Begley, A., Querel, R.: Surface and tropospheric ozone trends in the Southern Hemisphere since 1990: possible linkages to poleward expansion of the Hadley circulation, *Science Bulletin*, 64, 400–409, <https://doi.org/10.1016/j.scib.2018.12.021>, 2019.
- 900 Ludwig, J., Meixner, F. X., Vogel, B., and Forstner, J.: Soil-air exchange of nitric oxide: An overview of processes, environmental factors, and modelling studies, *Biogeochemistry*, 52, 225–257, DOI: 10.1023/A:1006424330555, 2001.
- Mari, C. H., Reeves, C. E., Law, K. S., Ancellet, G., Andres-Hernandez, M. D., Barret, B., Bechara, J., Borbon, A., Bouarar, I., Cairo, F., Commare, R., Delon, C., Evans, M. J., Fierli, F., Floquet, C., Galy-Lacaux, C., Heard, D. E., Homan, C. D., Ingham, T., Larsen, N., Lewis, A. C., Lioussse, C., Murphy, J. G., Orlandi, E., Oram, D. E., Sauniois, M., Serça, D., Stewart, D. J., Stone, D., Thouret, V., van
- 905 Velthoven, P. and Williams, J. E.: Atmospheric composition of West Africa: highlights from the AMMA international program, *Atmos. Sci. Let.* 12, 13–18, <https://doi.org/10.1002/asl.289>, 2011.
- Martins, J. J., Dhammapala, R. S., Lachmann, G., Galy-Lacaux, C., and Pienaar, J. J.: Long-term measurements of sulphur dioxide, nitrogen dioxide, ammonia, nitric acid and ozone in southern Africa using passive samplers, *S. Afr. J. Sci.*, 103, 336–342, <https://hdl.handle.net/10520/EJC96693>, 2007.
- 910 Mayaux, P., Bartholomé, E., Fritz, S., and Belward, A.: A new land-cover map of Africa for the year 2000: New land-cover map of Africa. *J. Biogeogr.*, 31, 861–877, <https://doi.org/10.1111/j.1365-2699.2004.01073.x>, 2004.
- Merabtene, T., Siddique, M., Shanableh, A.: Assessment of seasonal and annual rainfall trends and variability in sharjah city, UAE. *Adv. Meteorol*, 2016, 1–13, <https://doi.org/10.1155/2016/6206238>, 2016.
- Mills, G., Pleijel, H., Malley, C. S., Sinha, B., Cooper, O. R., Schultz, M. G., Neufeld, H. S., Simpson, D., Sharps, K., Feng, Z., Gerosa, G.,
- 915 Harmens, H., Kobayashi, K., Saxena, P., Paoletti, E., Sinha, V., and Xu, X.: Tropospheric Ozone Assessment Report: Present-day tropospheric ozone distribution and trends relevant to vegetation. *Elem Sci Anth*, 6, 1–46, DOI: <https://doi.org/10.1525/elementa.302>, 2018.
- Morakinyo, O. M., Mukhola M. S., and Mokgobu. M. I.: Ambient Gaseous Pollutants in an Urban Area in South Africa: Levels and Potential Human Health Risk. *Atmosphere*, 11, 1–14, doi:10.3390/atmos11070751, 2020.
- 920 Mouissi, S., Alayat, H.: (2016) Use of the Principal Component Analysis (PCA) for Physico-Chemical Characterization of an Aquatic Ecosystem Waters: Case of Oubeira Lake (Extreme Northeastern Algeria), *J. Mater. Environ. Sci.* 7, 2214–2220, 2016.
- Monks, P. S., Archibald, A. T., Colette, A., Cooper, O., Coyle, M., Derwent, R., Fowler, D., Granier, C., Law, K. S., Mills, G. E., Stevenson, D. S., Tarasova, O., Thouret, V., von Schneidmesser, E., Sommariva, R., Wild, O., and Williams, M. L.: Tropospheric ozone and its precursors from the urban to the global scale from air quality to short-lived climate forcer, *Atmos. Chem. Phys.*, 15, 8889–8973, <https://doi.org/10.5194/acp-15-8889-2015>, 2015.
- 925 Monks, P., Leigh, R.: Tropospheric chemistry and air pollution. In: Hewitt, C.N., Jackson, A.V. (Eds.), *Atmospheric Science for Environmental Scientists*. Wiley-Blackwell, Oxford, UK, 300 pp, ISBN 978140518542-4, 2009.
- Ngoasheng, M., Beukes, J. P., van Zyl, P. G., Swartz, J.-S., Loate, V., Krisjan, P., Mpambani, S., Kulmala, M., Vakkari, V., and Laakso, L.: Assessing SO₂, NO₂ and O₃ in rural areas of the North West Provinc. *Clean air journal*, 31, 1–14, <http://dx.doi.org/10.17159/caj/2021/31/1.9087>, 2021.
- 930



- Ojumu, A.M.: Transport of Nitrogen Oxides and Nitric Acid Pollutants over South Africa and Air Pollution in Cape Town. MSc, University of South Africa, 68 pp, 2013.
- Oltmans, S. J., Lefohn, A. S., Shadwick, D., Harris, J. M., Scheel, H. E., Galbally, I., Tarasick, D. W., Johnson, B. J., Brunke, E. G., Claude, H., Zeng, G., Nichol, S., Schmidlin, F., Davies, J., Cuevas, E., Redondas, A., Naoe, H., Nakano, T., and Kawasato, T.: Recent tropospheric ozone changes-A pattern dominated by slow or no growth, *Atmos. Environ.*, 67, 331–351, <https://doi.org/10.1016/j.atmosenv.2012.10.057>, 2013.
- 935 Oluleye, A., Satellite Observation of Spatio-temporal Variations in Nitrogen Dioxide over West Africa and Implications for Regional Air Quality, *Journal of Health & Pollution*, 11, 1–16, DOI: 10.5696/2156-9614-11.31.210913, 2021.
- Oluleye, A., and Okogbue, E. C.: Analysis of temporal and spatial variability of total column ozone over West Africa using daily TOMS measurements, *Atmospheric Pollution Research*, 4, 387–397, <https://doi.org/10.5094/APR.2013.044>, 2013.
- 940 Onojeghuo, A. R., Balzter, H., Monks, P. S.: Tropospheric NO₂ concentrations over West Africa are influenced by climate zone and soil moisture variability., *Atmos. Chem. Phys. Discuss.*, doi:10.5194/acp-2016-1128, 2017.
- Ossouhou M., C. Galy-Lacaux, C., V. Yoboué, V., Hickman, J. E., Gardrat, E., Adona, M., Darrasi, S., Laoualie, D., Akpod, A., Ouafo, M., Diop, B., Opepah, C.: Trends and seasonal variability of atmospheric NO and HNO concentrations across three major African biomes inferred from long-term series of ground-based and satellite measurements, *Atmos. Environ.* 207, 148–66, <https://doi.org/10.1016/j.atmosenv.2019.03.027>, 2019.
- Petäjä, T., Vakkari, V., Pohja, T., Nieminen, T., Laakso, H., Aalto, P. P., Keronen, P., Siivola, E., Kerminen, V.-M., Kulmala, M., and Laakso, L.: Transportable Aerosol Characterization Trailer with Trace Gas Chemistry: Design, Instruments and Verification, *Aerosol Air Qual. Res.*, 13, 421–435, <https://doi.org/10.4209/aaqr.2012.08.0207>, 2013.
- 950 Petetin, H., Bowdalo, D., Bretonnière, P.-A., Guevara, M., Armengol, J. M., Cabre, M. S., Serradell, K., Jorba, O., Soret, A., and Garcia-Pando, C. P.: Model output statistics (MOS) applied to Copernicus Atmospheric Monitoring Service (CAMS) O₃ forecasts: trade-offs between continuous and categorical skill scores, *Atmos. Chem. Phys.*, 22, 11603–11630, <https://doi.org/10.5194/acp-22-11603-2022>, 2022.
- 955 Rummel, U., Ammann, C., Kirkman, G. A., Moura, M. A. L., Foken, T., Andreae, M. O., and Meixner, F. X.: Seasonal variation of ozone deposition to a tropical rain forest in southwest Amazonia, *Atmos. Chem. Phys.*, 7, 5415–5435, doi:10.5194/acp-7-5415-2007, 2007.
- Sadiq, M., Tai, A. P. K., Lombardozzi, D., and Martin, M. V.: Effects of O₃-vegetation coupling on surface O₃ air quality via biogeochemical and meteorological feedbacks, *Atmos. Chem. Phys.* 17, 3055–3066. <https://doi.org/10.5194/acp-17-3055-2017>, 2017.
- Salem, A. A., Soliman, A. A., El-Haty, I. A.: Determination of nitrogen dioxide, sulfur dioxide, ozone, and ammonia in ambient air using the passive sampling method associated with ion chromatographic and potentiometric analyses, *Air Qual Atmos Health*, 2, 133–145, doi: 10.1007/s11869-009-0040-4, 2009.
- Saunio, M., Reeves, C. E., Mari, C., Murphy, J. G., Stewart, D. J., Mills, G. P., Oram, D. E., and Purvis, R. M.: Ozone budget in the West African lower troposphere during the African Monsoon Multidisciplinary Analysis (AMMA) campaign, *Atmos. Chem. Phys.*, 9, 6135–6155, doi:10.5194/acp-9-6135-2009, 2009.
- 965 Sauvage, B., Thouret, V., Cammas, J.-P., Gheusi, F., Athier, G., and Nédélec, P.: Tropospheric ozone over Equatorial Africa: regional aspects from the MOZAIK data, *Atmos. Chem. Phys.*, 5, 311–335, <https://doi.org/10.5194/acp-5-311-2005>, 2005.
- Saxton, J. E., Lewis, A. C., Kettlewell, J. H., Ozel, M. Z., Gogus, F., Boni, Y., Korogone, S. O. U., and Serca. D.: Isoprene and monoterpene measurements in a secondary forest in northern Benin, *Atmos. Chem. Phys.*, 7, 4095–4106, <https://doi.org/10.5194/acp-7-4095-2007>, 2007.
- 970 Schultz, M. G., et al.: Tropospheric Ozone Assessment Report: Database and metrics data of global surface ozone observations, *Elem Sci Anth*, 5, 1–26, DOI: <https://doi.org/10.1525/elementa.244>, 2017.
- Sen P., K.: Estimates of the regression coefficient based on Kendall's tau, *J. Am. Stat. Assoc.* 63, 1379–1389, <https://doi.org/10.2307/2285891>, 1968.
- Serca, D., Guenther, A., Klinger, L., Vierling, L., Harley, P., Druilhet, A., Greenberg, J., Baker, B., Baugh, W., Bouka-Biona, C., and Loemba-Ndombi, J.: EXPRESSO flux measurements at upland and lowland Congo tropical forest site, *Tellus B*, 53, 220–234, <https://doi.org/10.3402/tellusb.v53i3.16593>, 2001.
- Silva, S. J., & Heald, C. L.: Investigating Dry Deposition of O₃ to Vegetation, *J. Geophys. Res. Atmos.*, 123, 559–573. <https://doi.org/10.1002/2017JD027278>, 2018.
- 975 Sindelarova, K., Granier, C., Bouarar, I., Guenther, A., Tilmes, S., Stavrou, T., Müller, J.-F., U. Kuhn, U., P. Stefani, P., and W. Knorr, W.: Global data set of biogenic VOC emissions calculated by the MEGAN model over the last 30 years, *Atmos. Chem. Phys.*, 14, 9317–9341, <https://doi.org/10.5194/acp-14-9317-2014>, 2014.
- 980 Sofen, E. D., Bowdalo, D., and Evans, M. J., How to most effectively expand the global surface ozone observing network, *Atmos Chem Phys* 16, 1445–1457. DOI: <https://doi.org/10.5194/acp-16-1445-2016>, 2016.



- 985 Stewart, D. J., Taylor, C. M., Reeves, C. E., and McQuaid, J. B.: Biogenic nitrogen oxide emissions from soils: impact on NO_x and ozone over west Africa during AMMA (African Monsoon Multidisciplinary Analysis): observational study, *Atmos. Chem. Phys.*, 8, 2285–2297, doi:10.5194/acp-8-2285-2008, 2008.
- Swap, R. J., Annegarn, H. J., Suttles, J. T., King, M. D., Platnick, S., Privette, J. L., Scholes, R. J.: Africa burning: a thematic analysis of the southern African regional science initiative (SAFARI 2000), *J. Geophys. Res.* 108, 1–15, <https://doi.org/10.1029/2003JD003747>, 2003
- 990 Swartz, J.-S., van Zyl, P. G., Beukes, J. P., Galy-Lacaux, C., Ramandh, A., and Pienaar, J. J.: Measurement report: Statistical modelling of long-term trends of atmospheric inorganic gaseous species within proximity of the pollution hotspot in South Africa, *Atmos. Chem. Phys.*, 20, 10637–10665, <https://doi.org/10.5194/acp-20-10637-2020>, 2020a.
- Swartz, J.-S., Van Zyl, P. G., Beukes, J. P., Labuschagne, C., Brunke, E.-G., Galy-Lacaux, C., Pienaar, J. J., Portafaix, T.: Twenty-one years of passive sampling monitoring of SO₂, NO₂ and O₃ at the Cape Point GAW station, South Africa, *Atmospheric Environment* 222, 1–17, <https://doi.org/10.1016/j.atmosenv.2019.117128>, 2020b.
- 995 Tarasick, D., Galball, I. E., Cooper, O. R., Schultz, M. G., Ancellet, G., Leblanc, T., Wallington, T. J., Ziemke, J., Liu, X., Steinbacher, M., Staehelin, J., Vigouroux, C., Hannigan, J. W., Garcia, O., Foret, G., Zanis, P., Weatherhead, E., Petropavlovskikh, I., Worden, H., Osman, M., Liu, J., Chang, K.-L., Gaudel, A., Lin, M., Granados-Muñoz, M., Thompson, A. M., Oltmans, S. J., Cuesta, J., Dufour, G., Thouret, V., Hassler, B., Trick T., and Neu, J. L.: Tropospheric Ozone Assessment Report: Tropospheric ozone from 1877 to 2016, observed levels, trends and uncertainties, *Elem Sci Anth*, 7, 1–72. DOI: <https://doi.org/10.1525/elementa.376>, 2019.
- 1000 Tiitta, P., Vakkari, V., Croteau, P., Beukes, J.P., Zyl, P.G.V., Josipovic, M., Venter, A.D., Jaars, K., Pienaar, J.J., Ng, N.L., Canagaratna, M.R., Jayne, J.T., Kerminen, V.M., Kokkola, H., Kulmala, M., Laaksonen, A., Worsnop, D.R., Laakso, L., Chemical composition, main sources and temporal variability of PM₁ aerosols in southern African grassland. *Atmos. Chem. Phys.* 14, 1909–1927. <https://doi.org/10.5194/acp-14-1909-2014>, 2014.
- Tsuyuzaki, K., Sato, H., Sato, K. and Nikaido, I.: Benchmarking principal component analysis for large-scale single-cell RNA-sequencing, *Genome Biology*, 21, 1–17, <https://doi.org/10.1186/s13059-019-1900-3>, 2020.
- 1005 Vakkari, V., Beukes, J.P., Laakso, H., Mabaso, D., Pienaar, J.J., Kulmala, M., Laakso, L., 2013. Long-term observations of aerosol size distributions in semi-clean and polluted savannah in South Africa. *Atmos. Chem. Phys.* 13, 1751–1770. <https://doi.org/10.5194/acp-13-1751-2013>.
- Vet, R., Artx, R. S., Carou, S., Shaw, M., Ro, C., Aas, W., Baker, A., Bowersox, V. C., Dentener, F., Galy-Lacaux, C., Hou, A., Pienaar, J.J., 1010 Gillet, R., Forti, M. C., Gromov, S., Hara, H., Khodzher, T., Mahowald, N. M., Nickovic, S., Rao, P. S. P., Reid, N. W.: A global assessment of precipitation chemistry and deposition of sulfur, nitrogen, sea salt, base cations, organic acids, acidity and pH, and phosphorus, *Atmos. Environ.* 93, 3–100, <https://doi.org/10.1016/j.atmosenv.2013.10.060>, 2014.
- Vitolo, C., Di Giuseppe, F., D'Andrea, M.: Caliver: an R package for CALibration and VERification of forest fire gridded model outputs, *PLoS ONE*, 13, 1–18, <https://doi.org/10.1371/journal.pone.0189419>, 2018.
- 1015 Williams, J. E., Scheele, M. P., van Velthoven P. F. J., Cammas, J.-P., Thouret V., Galy-Lacaux, C., Volz-Thomas, A.: The influence of biogenic emissions from Africa on tropical tropospheric ozone during 2006: a global modeling study, *Atmos. Chem. Phys.*, 9, 5729–5749, <https://doi.org/10.5194/acp-9-5729-2009>, 2009.
- Young, P. J., Archibald, A. T., Bowman, K. W., Lamarque, J.-F., Naik, V., Stevenson, D.S., Tilmes, S., Voulgarakis, A., Wild, O., Bergmann, D., Cameron-Smith, P., Cionni, I., Collins, W. J., Dalsøren, S. B., Doherty, R. M., Eyring, V., Faluvegi, G., Horowitz, L. W., Josse, B., 1020 Lee, Y. H., MacKenzie, I. A., Nagashima, T., Plummer, D. A., Righi, M., Rumbold, S. T., Skeie, R. B., Shindell, D. T., Strode, S. A., Sudo, K., Szopa, S. and Zeng, G.: Corrigendum to “Pre-industrial to end 21st century projections of tropospheric ozone from the Atmospheric Chemistry and Climate Model Intercomparison Project (ACCMIP)”, *Atmos. Chem. Phys.*, 13, 2063–2090, *Atmos. Chem. Phys.*, 13, 5401–5402. DOI: <https://doi.org/10.5194/acp-13-5401-2013>, 2013.
- Young, P. J., Naik, V., Fiore, A. M., Gaudel, A., Guo, J., Lin, M. Y., Neu, J. L., Parrish, D. D., Rieder, H. E., Schnell, J. L., Tilmes, S., Wild, 1025 O., Zhang, L., Ziemke, J., Brandt, J., Delcloo, A., Doherty, R. M., Geels, C., Hegglin, M. I., Hu, L., Im, U., Kumar, R., Luhar, A., Murray, L., Plummer, D., Rodriguez, J., Saiz-Lopez, A., Schultz, M. G., Woodhouse M. T., and Zeng G.: Tropospheric Ozone Assessment Report: Assessment of global-scale model performance for global and regional ozone distributions, variability, and trends, *Elem Sci Anth*, 6, 1–49, DOI: <https://doi.org/10.1525/elementa.265>, 2018.
- Zhang, Y., Cooper, O. R., Gaudel, A., Thompson, A. M., Nédélec, P., Ogino, S.-Y. and West, J. J.: Tropospheric ozone change from 1980 to 1030 2010 dominated by equatorward redistribution of emissions. *Nature Geoscience* 9, 875–879, DOI: <https://doi.org/10.1038/ngeo2827>, 2016.
- Zunckel M., Venjonoka K., Pienaar J. J., Brunke E. G., Pretorius O., Koosiale A., Raghunandan A., van Tienhoven A. M., Surface ozone over southern Africa: synthesis of monitoring results during the cross-border air pollution impact assessment project. *Atmos Environ.* 38:6139–6147. doi:10.1016/j.atmosenv.2004.07.029, 2004.
- 1035 Zwarts, L., Bijlsma, R. G., and Kamp, J.: Selection by Birds of Shrub and Tree Species in the Sahel, *Ardea*, 111, 143–174, <https://doi.org/10.5253/arde.2022.a20>, 2023.